The Effect of Distribution Transformers on Carrier Signal Propagation for a Power Distribution Line at Power Line Carrier Frequencies

Rodney C. Hemminger

Center for Communications and Signal Processing
Dept. of Electrical and Computer Engineering
North Carolina State University
Raleigh, NC

April 1985

CCSP-TR-85/8

ABSTRACT

HEMMINGER, RODNEY C. The effect of distribution transformers on carrier signal propagation for a power distribution line at power line carrier frequencies. (Under the direction of Dr. J. B. O'Neal)

A distributed model of a power distribution line with distribution transformers was developed. A brief investigation into the primary impedance range of distribution transformers for frequencies from 1 to 50-kHz was made. This impedance was found to be quite high and predominately capacitive in nature. The effect of the distribution transformers on the propagation constant and the characteristic impedance was determined for two cases of secondary loading.

Two sets of signal propagation measurements were made. The first dealt with the propagation characteristics of the distribution line in the frequency domain with and without transformers. The second set of measurements was concerned with the attenuation of the signal with distance along the line. These measurements resulted in several plots of actual standing-waves on the distribution line. These measurments were also performed with transformers attached to the distribution line. Attenuation was minimal with the addition of the transformers.

ACKNOWLEDGEMENTS

The author wishes to thank Dr. J. B. O'Neal of North Carolina State University; Kay Clinard, Lou Gale, and the other members of the Design Research Unit of Distribution Engineering at Carolina Power and Light Company; and Ken Shuey of Westinghouse Electric Corporation for their invaluable assistance and support of this research.

TABLE OF CONTENTS

LIST OF FIGURES

LIST OF FIGURES (Cont'd)

LIST OF FIGURES (Cont'd)

LIST OF SYMBOLS

Hz	Hertz
kHz	Kilohertz
PLC	Power Line Carrier
DLC	Distribution Line Carrier
nF	Nanofarad
kV	Kilovolt
KVA	Kilovolt-Amp
kohm	Kilohm
AWG	American Wire Gauge
Zo	Characteristic Impedance
L	Inductance
C	Capacitance
uH	Microhenry
uF	Microfarad
m	meter
f	Frequency
pi	3.1415926...
dB	Decibel
dBV	Decibel Referenced to One Volt
dBm	Decibel Referenced to One Milliwatt
dBohm	Decibel Referenced to One Ohm
msec	millisecond
usec	Microsecond

LIST OF SYMBOLS (Cont'd)

V	Volt
sec	Second
R	Resistance
j	Square Root of -1
H	Henry

1. INTRODUCTION

Over the past several years, electric utility companies have found themselves under mounting pressure to make more efficient use of their existing facilities. The regulatory process controlling the construction of new nuclear power plants and the stringent environmental regulations governing coal fired plants are combining to slow the rate of new plant construction. High interest rates and a lower demand for electricity are also contributing factors to construction delays.

The importance of Distribution Line Carrier technology continues to increase as utility companies look toward load management and distribution automation schemes as viable alternatives to the construction of new generating plants at previous growth rates. Load management and distribution automation are two methods of lowering and controlling the peak demand and saving energy, especially distribution losses. Substantial research has been done in the past decade on the comparison of different communications alternatives for an automated distribution network [2,5]. Such a system relies on a bi-directional communications link between the central controlling facility and thousands of points spread out over the distribution feeder.

Distribution Line Carrier (DLC) is one of the more promising communications technologies for such a system [5]. DLC systems inject a carrier signal (currently in the 2-kHz to 20-kHz range) directly onto the distribution lines. A significant advantage of DLC is that the communication's medium is already in place and owned by the utility company, in addition to having an exceptionally high reliability. Several manufacturers now have commercial DLC systems on the market.

Before a new communication technology can be used to its full potential, a complete understanding of the channel's propagation characteristics is necessary. Power distribution systems have yet to be completely characterized at DLC frequencies. As one might expect, the power distribution network is a very harsh environment for DLC signals. The distribution feeder is a constantly changing physical and electrical environment. Several sources of uncertainty are encountered for signal paths on a typical distribution feeder. Changing transformer secondary loads, feeder configurations (due to new construction or feeder switching), and noise levels are just a few of these uncertainties. Additionally, the individual components of the distribution network may have widely varying characteristics at DLC frequencies.

The first part of this paper is devoted to the development of a distributed model for a power distribution line that includes the effects of distribution transformers and their secondary loads. As this paper is primarily intended for engineers in the utility environment, a short section on the relevant transmission line theory is included for the convienence of the reader. A brief analysis of the primary impedance range for distribution transformers was necessary to simplify the results and is also included in this section. The model will be based on the standard distributed model for a two-wire transmission line. Important propagation parameters, such as the characteristic impedance and the propagation constant, are discussed in detail for a single-phase overhead line.

Carrier signal propagation measurements are then made to justify the results of the first section. It is no easy task to obtain a controlled environment for measurements on actual distribution lines. The many sources of uncertainty and the physical constraints of a high-voltage environment severely limit measurement capability. This lack of a controlled test environment has hindered an understanding of the distribution feeder as a communications medium. Carolina Power and Light Co. recently completed a Distribution Test Facility near Raleigh, N.C. [16]. This test facility (including a substation and over 15 miles of overhead and underground distribution lines) was used extensively in measuring carrier signal propagation.

Measurements of signal propagation were made on a single-phase overhead line, and then repeated with distribution transformers attached to the line. These measurements permit a comparison of the distributed model's results to the measured changes in carrier signal propagation.

2. Distributed Model

Distribution Line Carrier is still a relatively new communications technology, and should not be confused with transmission line carrier (which has been in use for over fifty years). An important step is being made in the design of these DLC systems. The system is centered around a transmission medium designed for an entirely different purpose, the distribution of 60-Hz power. Before one can specify what modulation technique is best suited for DLC, some basic research must done on the characteristics of the transmission medium. Although extensive data is available for distribution systems at 60 Hz, the picture is not completely defined at carrier frequencies in the VLF range (used by current DLC systems).

One goal of this paper is to make a simplification of the distribution system at DLC frequencies by incorporating the distribution transformers (and their respective secondary loads) into a distributed model of the distribution line. Research in this area is important in establishing a fundamental understanding of the power distribution network at DLC frequencies. Distribution transformers and the lines themselves create almost the entire transmission medium. Research will probably never result in the obtaining a uniform constant carrier attenuation in dB per unit distance. There are just too many possibilities for different line conditions in a distribution feeder to obtain a completely consistent result. Such factors include line branches, transformer size, transformer spacing, three-phase conductor spacing and configuration, and multiple signal paths. However, developing a greater understanding of the how the elements of a distribution system affect carrier signal propagation is still vital to the development of an optimal DLC system.

In order to accomplish this goal, a distributed model of a single-phase distribution line and it's associated transformers is postulated. In developing this model, transmission line theory is applied to a single-phase power distribution line. The equations generated are then modified to incorporate the effect of the distribution transformers and their secondary loads. It is anticipated that the results for the single-phase line to apply for three-phase distribution lines as well.

2.1 Single-Phase Distribution Line

The theory concerning propagation characteristics for transmission lines has been well documented in the previous years. This theory is now applied to a power distribution line, noting the discrepancies between the distribution line and an ideal transmission line. A brief summary of the relevant derivations are included here as a review of the classical model before presenting the postulated model.

The basic transmission line equations are derived by first considering a short length of a uniform two-conductor line. A circuit equivalent to this short length of transmission line is shown in figure 2.1 [4,6].

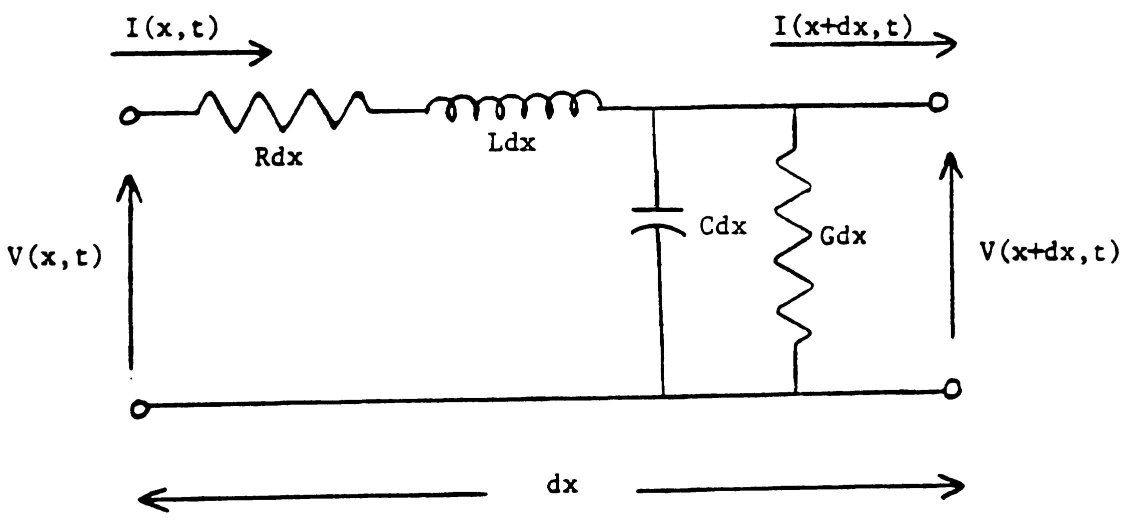

Figure 2.1 - Classical RLCG distributed circuit model

The R, L, C, and G parameters are expressed per unit length. For the scope of this paper their dimensions are defined as follows: R in ohms/mile, L in henries/mile, C in farads/mile, and G in mhos/mile. Voltage and current along the line can be expressed a function of the distance x, and are [4]

$$\frac{dV(x)}{dx} = -I(x)(R + j\omega L) \tag{2.1}$$

$$\frac{dI(x)}{dx} = -V(x)(G + j\omega C) \tag{2.2}$$

By solving these equations for V(x) and I(x), it can be shown that [4,13]

$$V(x) = Ae^{-\gamma x} + Be^{\gamma x} \tag{2.3}$$

$$I(x) = \left[\frac{G + j\omega C}{R + j\omega L}\right]^{\frac{1}{2}}(Ac^{-\gamma x} - Be^{\gamma x}) \tag{2.4}$$

These equations describe two waves traveling along the line in opposite directions, with the propagation constant gamma given by

$$\gamma = \{(R + j\omega L)(G + j\omega C)\}^{\frac{1}{2}} \tag{2.5}$$

The impedance seen by a forward traveling wave (or a backward traveling wave) is defined as the characteristic impedance Zo. Comparing the like terms of equations 2.2 and 2.4 shows that Zo is

$$Z_o = \left[\frac{R + j\omega L}{G + j\omega C}\right]^{\frac{1}{2}} \qquad (2.6)$$

It is quite important to understand the consequences of the presence of forward and backward traveling waves. Consider the measured voltage at some point P along the line [13].

$$V_p = |V(x)| = |Ae^{-\gamma x}||1 + ke^{2\gamma x}| \qquad (2.7)$$

Here, k represents the reflection coefficient, defined as k = B/A [13]. In general k will be complex, and taking

$$k = Ke^{j\theta} \qquad (K < 1) \qquad (2.8)$$

it can be shown for a lossless line (alpha equal to zero) that

$$V_p = A\{1 + K^2 + 2K\cos(2\beta x + \theta)\}^{\frac{1}{2}} \qquad (2.9)$$

This expression is illustrated in figure 2.2 [13].
Note that Vp varies between a maximum of A(1 + K) and a minimum of A(1 - K). Furthermore, Vp is periodic with a

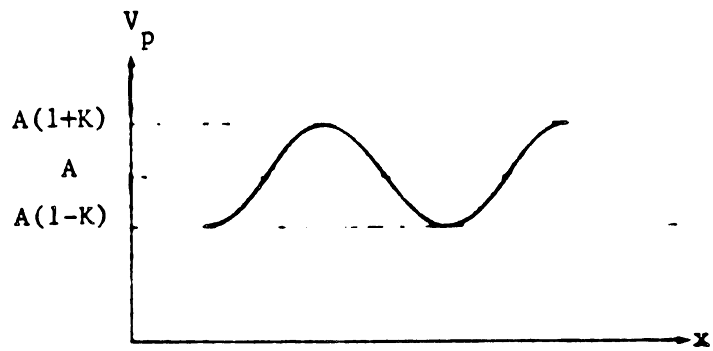

Figure 2.2 - Standing-wave pattern for a partial reflection on a lossless line

period determined by 2Bx = 2(pi), or x = .5 lambda [4].

When K = 1, the voltage drops to zero at the minima and the standing-wave pattern takes on the more familiar shape of figure 2.3 [13]. This is the pattern exhibited by a pure standing wave.

The more general case of a lossy line (alpha is no longer constrained to be equal to zero) is slightly more complicated. The measured voltage is represented by [13]

$$V_p = Ae^{-\gamma x}\{1 + K^2 e^{4\gamma x} + 2Ke^{2\gamma x}\cos(2\beta x + \theta)\}^{\frac{1}{2}} \qquad (2.10)$$

As alpha approaches zero, this reduces to equation 2.9. When alpha becomes significant, the reflected wave will decay resulting in a standing-wave pattern similiar to

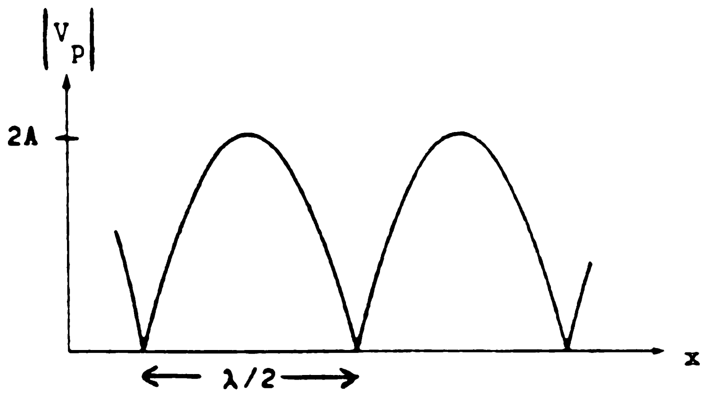

Figure 2.3 - Standing-wave pattern for a complete reflection on a lossless line

figure 2.4 [13].

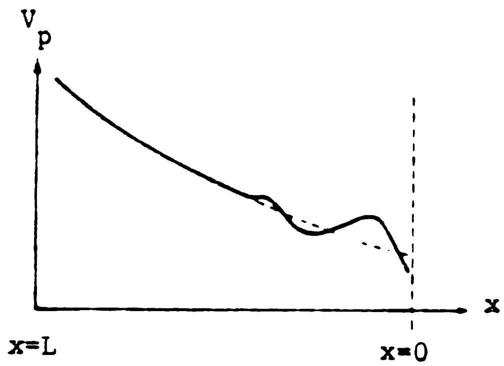

Figure 2.4 - A typical standing-wave pattern for a lossy line

In figure 2.4, $x = 0$ is the point of reflection, and $x = -L$ is the source.

At this point, no deviations have been made from what is considered standard transmission line theory. Before considering the effect distribution transformers have on these equations, it is important to consider the validity of applying this theory to a single — phase power distribution line.

The incremental transmission line model can easily be used to represent a section of a power distribution line with one notable exception. In the distribution system, the neutral line is grounded at every pole. This makes for a more complicated return path, and is not consistent with figure 2.1. In order to determine the significance of this discretely-connected ground plane, the per mile capacitance of an unconnected distribution line was measured. A 20,847 ft. section of distribution line was isolated at Carolina Power and Light Co.'s Distribution Test Site. Both ends of this section were open-circuited and nothing was attached to the line. The line's capacitance between phase and neutral was then measured with a Doric C-meter (model 130-A). Measuring the capacitance over a one-hour period demonstrated that the capacitance varied slightly with time. Values as high as 42 nanofarads and as low as 30 nanofarads were measured. However, over 90 percent of the time the capacitance was between 33 and 35 nanofarads. This 33 to 35 nanofarad range corresponds to 8.4 to 8.5 nanofarads per mile. One pointer to the validity of applying transmission line theory for two parallel lines to the power distribution line is whether the capacitance of the line can be accurately predicted by considering the distribution line as two parallel lines.

It can be shown that the capacitance between two parallel wires is

$$C = \frac{0.01941}{\log \frac{D}{r}} \quad \mu F/mile \tag{2.11}$$

where D is the distance between the two wires and r is the radius of the wires [18]. At the Distribution Test Site, both the phase and neutral lines are #2 aluminum, with a diameter of .2576 inches [9]. The spacing between phase and neutral is generally 3 ft., but increases to as much as 10 ft. in places. Equation 2.11 is relatively insensitive to small changes in either D or r since only the logarithm of their ratio appears. Taking D = 4-ft. results in an expected capacitance of 7.5 nanofarads per mile. This is slightly lower than the measured value but is quite close. For comparison purposes, consider the capacitance between a single wire and a plane (in this case the physical ground surface). A similiar equation for this capacitance can be derived and is [8]

$$C = \frac{0.03882}{\log \left(\frac{2h}{r}\right)} \quad \mu F/mile \tag{2.12}$$

where h is the height between the line and the plane. Generally, the phase line is between 25 and 30 ft. above the ground, but at times it is as high as 55-ft. above the ground. Once again, this change in height does not have a large effect on the expected capacitance because of the logarithmic ratio. Considering the single – phase distribution line as a single line 30-ft. above a ground plane, a capacitance of 10.4 nanofarads per mile would be expected. This expected value for the capacitance brackets the measured value on high side. The measured capacitance is closer to what is expected from two parallel wires, so the assumption is made that it is reasonable to approximate the distribution line by two parallel wires. This assumption will be substantiated with the presentation of propagation measurements in a later section.

The distributed parameter network of figure 2.1 will now be directly applied to a distribution line and provisions will be made to incorporate the effect of the distribution transformers. The propagation constant and the characteristic impedance are two of the more important characteristics in terms of characterizing the propagation of carrier signals. For this reason, the effect of the transformers on these characteristics will be the primary concern.

2.2 Distribution Line with Transformers

The necessary background has now been laid and the next step is to consider the effects of distribution transformers. On a given feeder, there may be more than a thousand transformers connected to the distribution line. In urban areas, there may be a transformer every 300 or 400 ft., whereas the spacing may be as large as a half-mile in rural areas. However, for any such area of a distribution system, the spacing between transformers remains relatively constant. This idea leads to the postulation of a "transformers per mile" characteristic for a given feeder or feeder section, and in turn treats the transformers as being somewhat evenly distributed along the distribution line. More importantly, the effects of each individual transformer are considered as being uniformly spread out along the section of line near it's location, instead of being a point discontinuity. With these assumptions in mind, the derivations for the resulting new characteristic impedance and propagation constant are presented.

The primary impedance of a single distribution transformer is a complex impedance, represented here by Zt. This impedance is, in general, a function of frequency, secondary load, transformer size, and possibly manufacturer. Assuming the impedance of the transformers is known, circuit parameters representing the transformers are inserted into the distributed model of the line. Let us assume the spacing of the transformers is given as N transformers per mile. The impedance contributed by the transformers on a per mile basis is then Zt/N since these impedances are added in parallel and are assumed to be equal. The per mile shunt admittance added by the transformers is then

$$Y_t = \frac{N}{Z_t} = G_t N + jX_t N \qquad (2.13)$$

The primary impedance of a distribution transformer consists of both a real and a reactive part. The circuit equivalent of a short length of "uniform" two conductor line is modified to obtain figure 2.5.
In addition to the original R, L, C, and G parameters, there are two new shunt elements representing the primary admittance of the distribution transformers.

In the general case, the voltage and the current along the line may be expressed as a function of the distance x

$$\frac{dV(x)}{dx} = -I(x)Z_s(j\omega) \qquad (2.14)$$

$$\frac{dI(x)}{dx} = -V(x)Y_p(j\omega) \qquad (2.15)$$

where Zs(jw) is the series impedance per unit length and

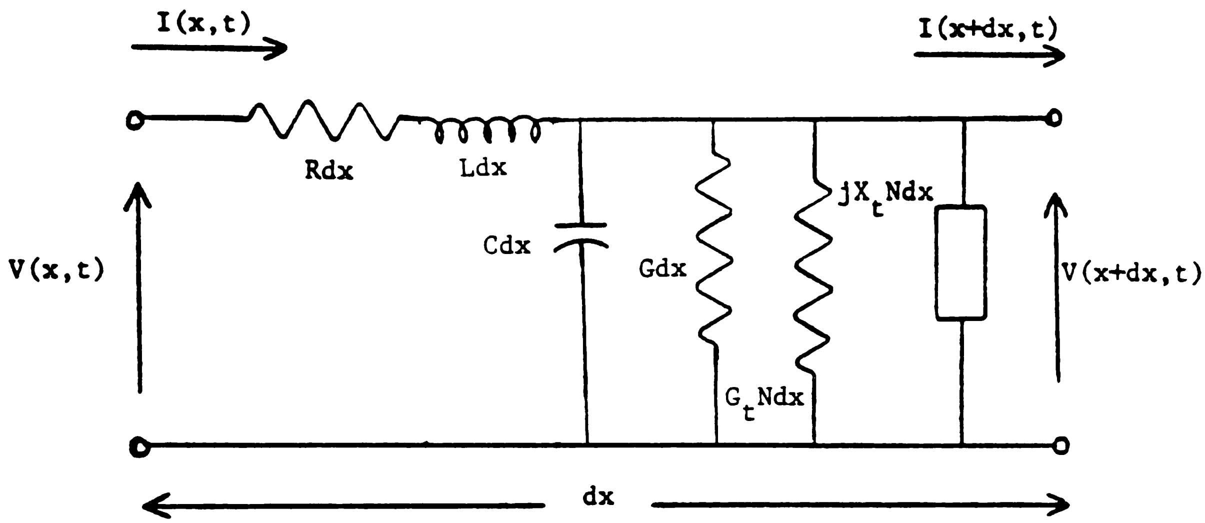

Figure 2.5 - Distributed model modified to include N distribution transformers per mile

Yp(jw) is the shunt admittance per unit-length. Note that the transformers are included into the model by a simply alteration of Yp(jw). Equations 2.14 and 2.15 are solved for V(x) and I(x) with Yp(jw) including the new shunt elements Gt*N and jXt*N to obtain

$$V(x) = Ae^{-\gamma' x} + Be^{\gamma' x} \tag{2.16}$$

$$I(x) = \left[\frac{(G + G_tN) + j\omega(C + X_tN)}{R + j\omega L}\right]^{\frac{1}{2}} \left[Ae^{-\gamma' x} - Be^{\gamma' x}\right] \tag{2.17}$$

where we now have

$$\gamma' = \{(R + j\omega L)(G + G_tN + j\omega(C + X_tN/\omega))\}^{\frac{1}{2}} \qquad (2.18)$$

and

$$Z_o' = \left[\frac{R + j\omega L}{(G + G_tN) + j\omega(C + X_tN/\omega)}\right]^{\frac{1}{2}} \qquad (2.19)$$

The effect of the transformers can be seperated from the effects of the line by expressing Zo' in terms of Zo. The same procedure is also done with the propagation constant. Considering the characteristic impedance first, a constant Ko is desired such that Zo' = Ko*Zo. Solving for Ko and simplifing yields

$$K_o = \left[\frac{G + j\omega C}{(G + G_tN) + j\omega(C + X_tN/\omega)}\right]^{\frac{1}{2}} \qquad (2.20)$$

Clearly, the addition of N transformers per mile results in the characteristic impedance being multiplied by the factor Ko. When N is zero, Ko simplifies to 1, and the characteristic impedance remains unchanged. For the propagation constant, a constant Ao is desired such that gamma' = Ao*gamma. Solving for Ao shows that Ao is identically equal to the inverse of Ko.

This separation of the transformer's effects from the original characteristics of the line has resulted in

$$Y' = \frac{1}{K_o} Y \tag{2.21}$$

$$Z_o' = K_o Z_o \tag{2.22}$$

where Ko is given in equation 2.20. In examining Ko, it becomes apparent that the effects of the transformers rests on the magnitudes (and phases) of N*Xt and N*Gt relative to C and G, respectively. Further generalizations or simplications of Ko depend on a knowledge of the primary impedance ranges that a distribution transformer may present to the distribution line. In the next section, a brief investigation is made into the primary impedance of distribution transformers.

2.3 Distribution Transformer Primary Impedance

Only a small amount of research has been done concerning the primary impedance of distribution transformers in the VLF range. In addition to knowing what impedance to expect, it is also quite important to understand the sensitivity of the primary impedance to transformer size, secondary load, and even manufacturer.

Measurement and modelling of distribution transformer primary impedance has been accomplished by two different approaches. One approach has been the use short-circuit admittance parameters (commonly known as the y parameters). The interested reader is referred to reference [17] for a complete discussion of this two-port parameter. A few studies have measured and analyzed the primary impedance (or admittance) using the y parameters [11,14]. A second approach involves the development of a simple RLC (see figure 2.6) plus ideal transformer circuit model that would adequately describe the primary impedance up to 50-kHz [12]. Both approaches have yielded essentially the same results. A brief summary of the results is presented in what follows (for more detail the reader is referred to references [11,14]).

In all cases the magnitude of the primary impedance is quite large, on the order of 10 kilohms or more. Above 25 kHz, the magnitude gradually decreases, but generally remains above 10 kilohms to beyond 50-kHz. The magnitude has a low Q resonance that usually falls in the 5 to 15-kHz range. Somewhat surprisingly, the phase of the primary impedance is predominately capacitive above 10-kHz. A peak in the phase plot occurs in the 2 to 10-kHz range. Note that this phase peak slightly precedes the magnitude resonance in the frequency domain. The impedance phase angle reaches a maximum at the point of resonance, and this maximum usually stays below 30 degrees. Once past the point of resonance, the phase angle drops sharply to below -80 degrees and remains almost completely capacitive out past 100 kHz. Most importantly, the phase angle usually becomes capacitive somewhere between 5 and 10 – kHz. Initially, this would imply that for DLC frequencies, the primary impedance of distribution transformers would be capacitive in nature.

For the purposes of this paper, it is important to know the range of values that the primary impedance may take. In order to accomplish this, an RLC plus ideal transformer model was implemented in software. This step was determined necessary to bound the primary impedance for varying secondary loads. Previous studies have used only resistive networks to represent secondary loads, and it was important to extend this to a completely general secondary load. The same RLC plus ideal transformer model that was presented by reference [12] is used. This model has been previously shown accurate for frequencies up to 50-kHz and is shown in figure 2.6 [11,7].

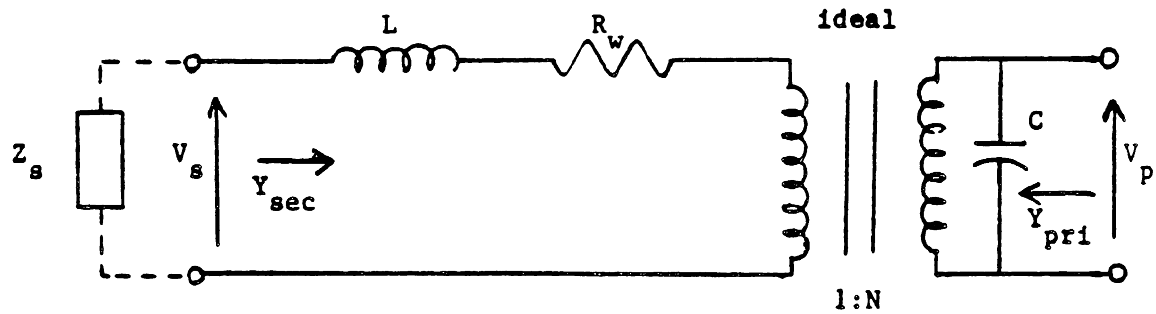

Figure 2.6 - Lumped parameter model of a distribution transformer

The transformer is ideal with a turns ratio of N:1 from the primary to the secondary side. Rw represents the winding resistance of the transformer's coils and L the leakage inductance present in the transformer. Zs is the secondary load. A single capacitor is used in shunt across the primary to represent the stray bushing and inter-winding capacitance. With this model, the primary impedance is given by equation 2.23.

$$Z_{in} = \frac{N^2(Z_s + R_w + j\omega L)}{1 + j\omega C N^2(Z_s + R_w + j\omega L)} \quad (2.23)$$

Extensive measurements concerning the Rw, L, and C parameters of this model have already been performed in reference [11], and the mean values of these parameters are listed in Table 2.1. The R value shown in Table 2.1 is not the same as Rw. Rw is a frequency dependent value, and

Table 2.1 - Mean values of the R, L, and C parameters of the distribution transformer model [11]

Transformer Size (kVA)	R (ohms)	L (mH)	C (nF)
10	.58	.16	.56
15	.54	.123	.90
25	.18	.075	.95
37.5	.16	.046	.83
50	.17	.045	.74
75	.12	.024	1.91
100	.08	.022	1.40

equation 2.24 approximates the relationship between R and Rw for the frequencies of interest [11]

$$R_w = \{\frac{R}{.14}\}\{\frac{f}{20\ kHz}\}^{1.4} \tag{2.24}$$

(the interested reader is referred to reference [11], pages 4-44 to 4-84 for a complete discussion on the determination of these values). R is a dummy parameter.

A brief program was written to calculate the possible primary impedance range for a distribution transformer using the lumped-parameter model shown in figure 2.6. In order to determine the possible primary impedance range, each of the Rw, L, and C parameters were varied through one standard deviation about their mean. Transformer size, turns ratio, and secondary load limits were established by the user. The resulting ranges for both the magnitude and phase could then be plotted against frequency. Initially, graphs were produced to show the sensitivity of the impedance to the Rw, L, and C parameters using this model. Figures 2.7 and 2.8 show the magnitude and phase ranges for a 10-KVA transformer with the secondary load held constant. The phase angle is scaled in degrees while the magnitude is scaled in dBohm. Here, dBohm is taken to mean 20 log(impedance/1 ohm). The limits on the secondary load are defined in terms of the load's power factor and percentage of full load at 60 Hz. Note that full load is determined by the KVA size of the transformer (the secondary voltage is assumed to be 240 volts line-to-line). In figures 2.7

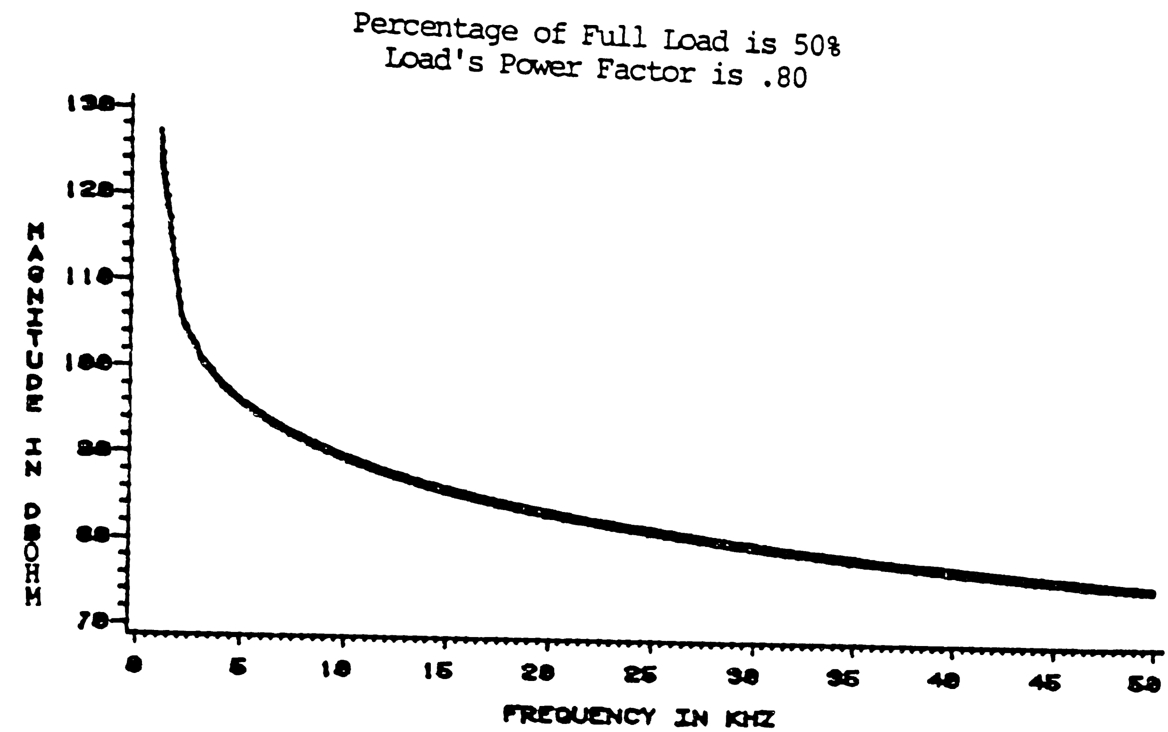

Figure 2.7 - Primary impedance magnitude for a half loaded 10-KVA distribution transformer

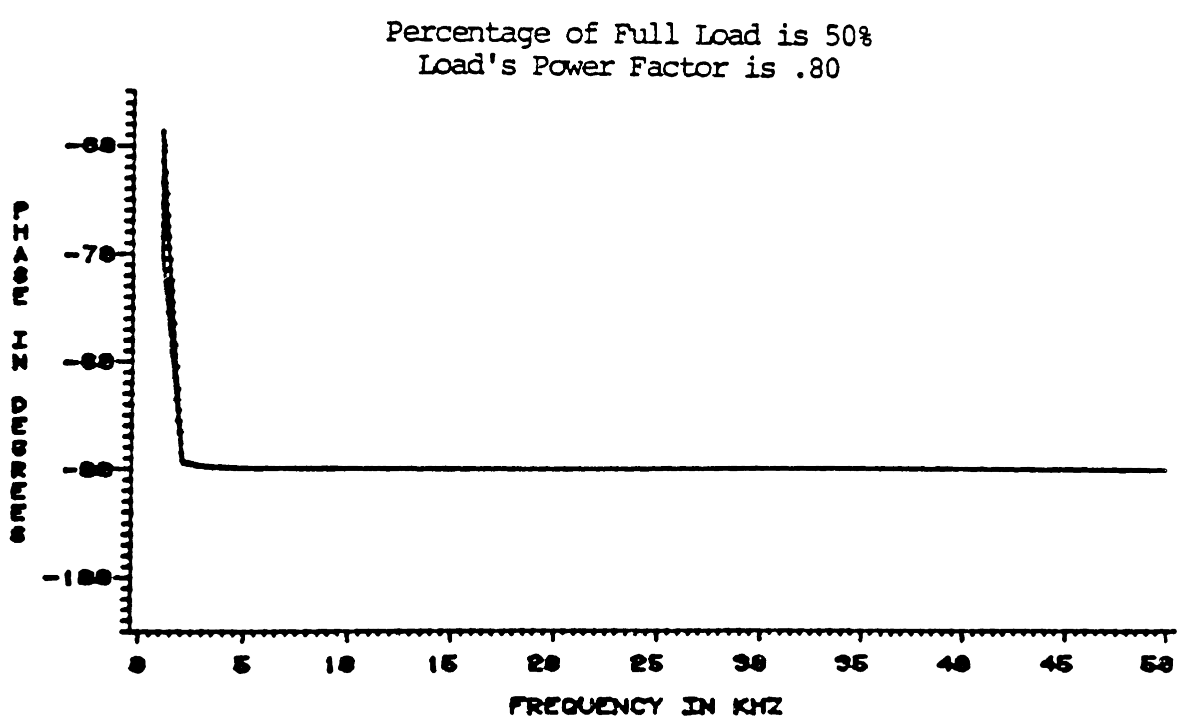

Figure 2.8 - Primary impedance phase for a half loaded 10-KVA distribution transformer

Percentage of Full Load is 50%
Load's Power Factor is .80

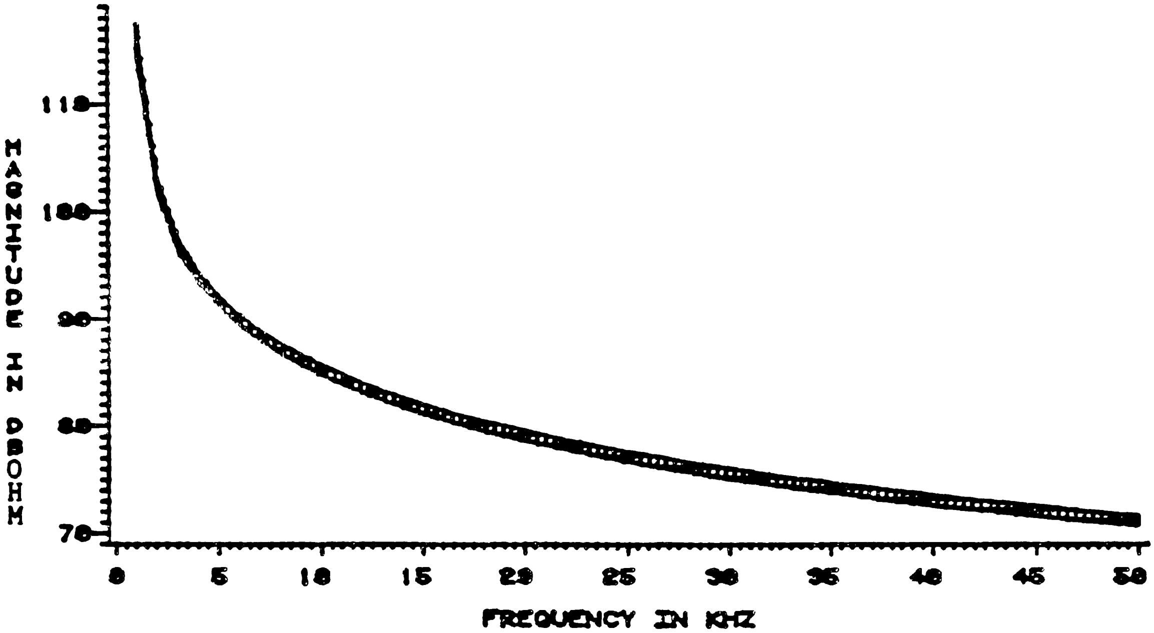

Figure 2.9 - Primary impedance magnitude for a half loaded 25-KVA distribution transformer

Percentage of Full Load is 50%
Load's Power Factor is .80

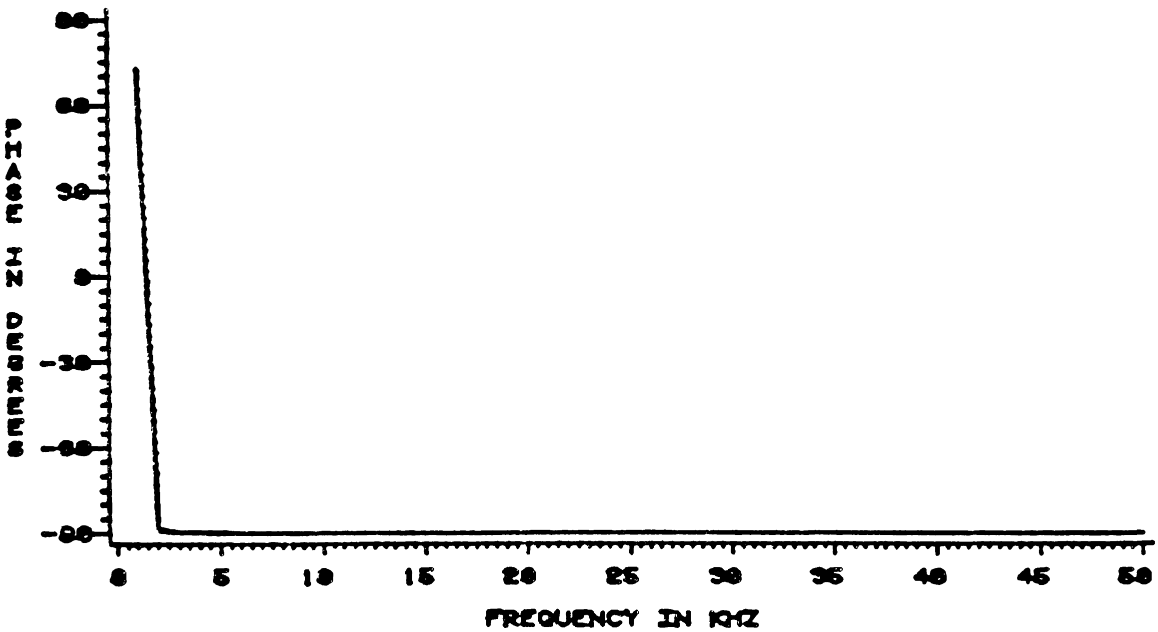

Figure 2.10 - Primary impedance phase for a half loaded 25-KVA distribution transformer

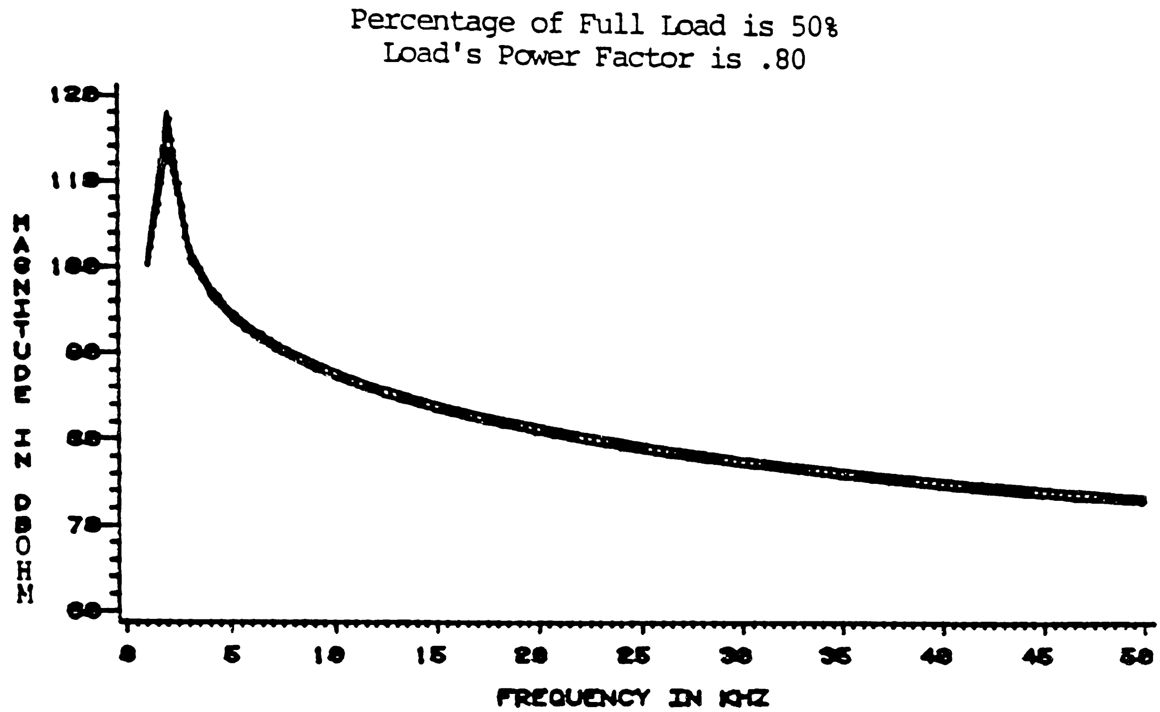

Figure 2.11 - Primary impedance magnitude for a half loaded 50-KVA distribution transformer

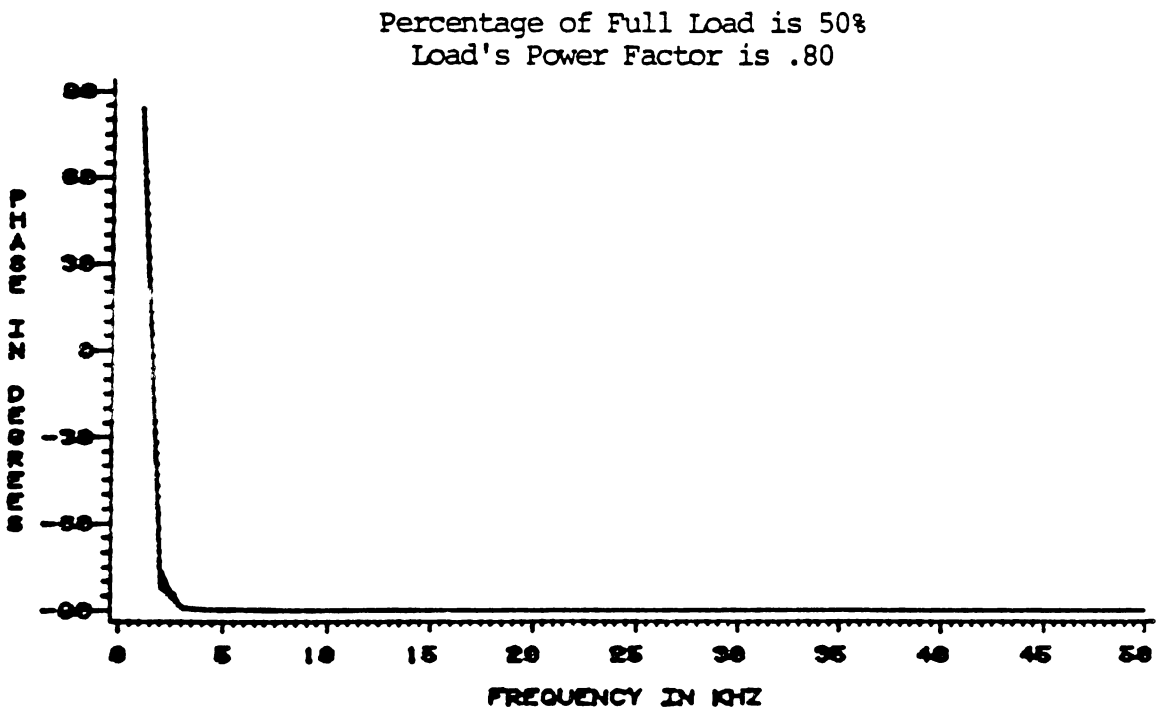

Figure 2.12 - Primary impedance phase for a half loaded 50-KVA distribution transformer

and 2.8 the secondary load is held constant at 50 percent of full load with a power factor of .8 (therefore designating an inductive, half-load situation). For both the magnitude and phase, the range of possible values is very small at all frequencies shown. It is therefore reasonable to infer that the impedance is relatively insensitive to variations in Rw, L, or C. Figures 2.9 through 2.12 contain the same information for 25-KVA and 50-KVA transformers, respectivly. It is interesting to note that for this particular secondary loading, the impedance is completely capacitive beyond 3 or 4 – kHz, regardless of transformer size. The magnitude of the impedance is very large at the lower frequencies, and a resonant peak is seen only for the 50-KVA transformer. Above 5-kHz the magnitude is very similiar for each of the transformers. All three drop from around 100 kilohms at 5 kHz, down to approximately 10 kilohms above 25 – kHz. For this particular case of secondary loading, the transformer size does not seem to appreciably affect the magnitude of the primary impedance.

Now that the effects of allowing the Rw, L, and C parameters to deviate from their respective means is known, the secondary load can be changed. Both the magnitude and the phase angle of the secondary load are varied. The magnitude ranges from 1 to 100 percent of full load while the power factor is varied from .4 to unity. These ranges are chosen as it has been determined that with few exceptions, normal secondary loads were within these limits [3].

The resulting primary impedance ranges for the magnitude and phase of a 10-KVA transformer are shown in figures 2.13 and 2.14, respectively. The upper and lower limits do not necessarily correspond to a particular secondary load because of possible interplay between between the Rw, L, and C parameters of the transformer with the secondary load's characteristics. For this reason, no assumptions are made concerning which secondary load causes the impedance limits for a given frequency. Notice that the possible range for the magnitude of the impedance has increased. This is especially true below 4 - kHz, where a range of 30 dB or so is possible. However, the shape and the relative magnitude of the impedance has not changed significantly (as compared with figure 2.7). This leads to the conclusion that the secondary load can influence the magnitude of the primary impedance, however this influence does not appear to be significant at frequencies above 5 kHz. Most important, however, is that this secondary load range always resulted in the magnitude of the primary

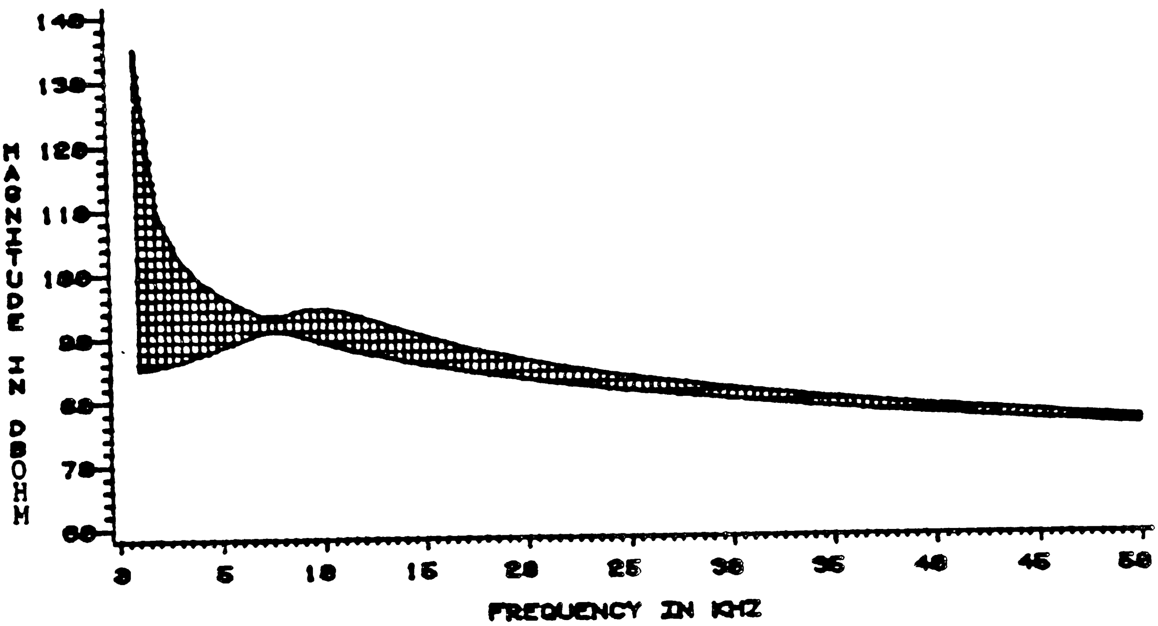

Figure 2.13 - Primary impedance magnitude range for a 10-KVA transformer

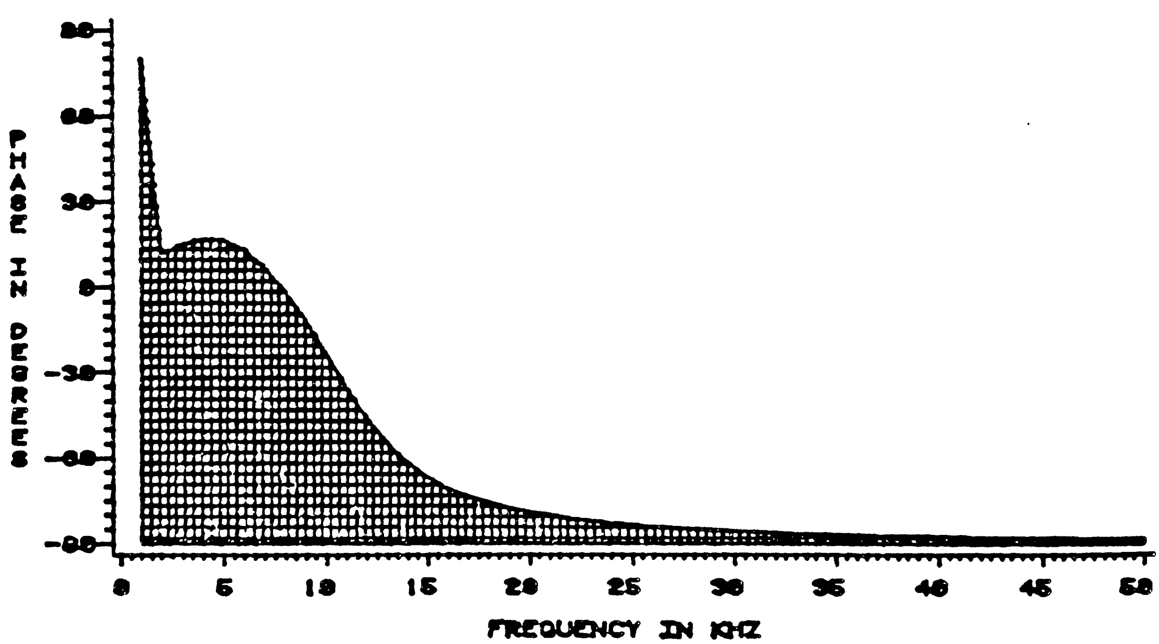

Figure 2.14 - Primary impedance phase range for a 10-KVA transformer

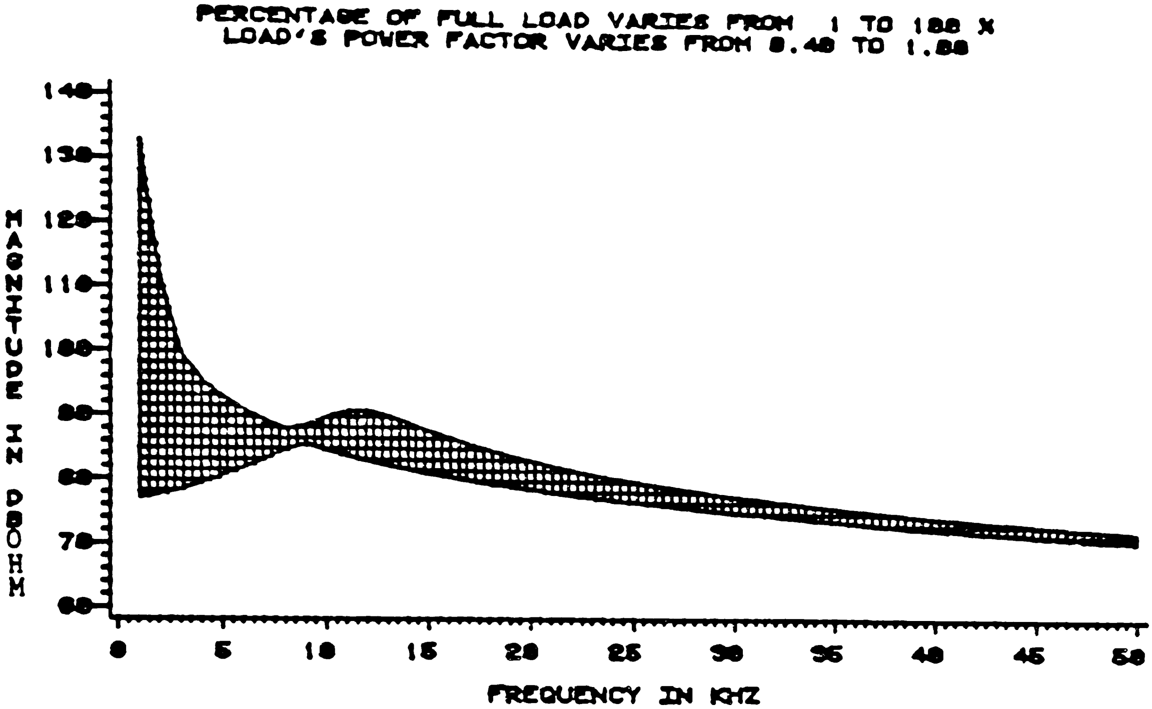

Figure 2.15 - Primary impedance magnitude range for a 25-KVA transformer

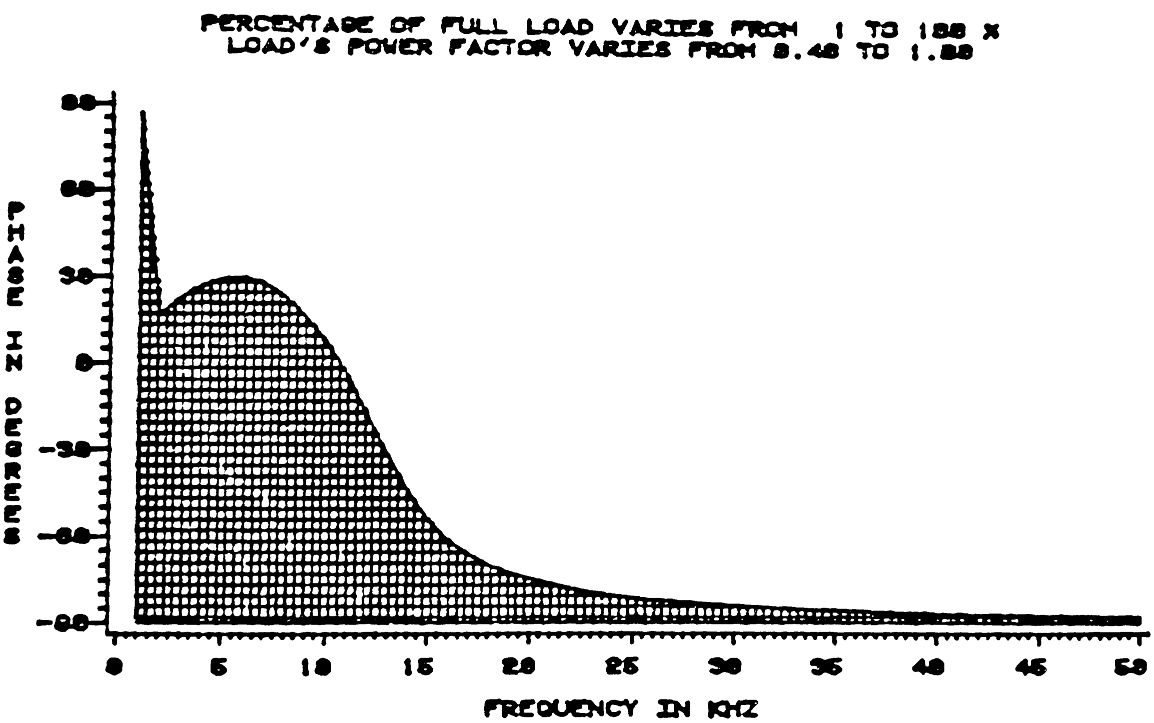

Figure 2.16 - Primary impedance phase range for a 25-KVA transformer

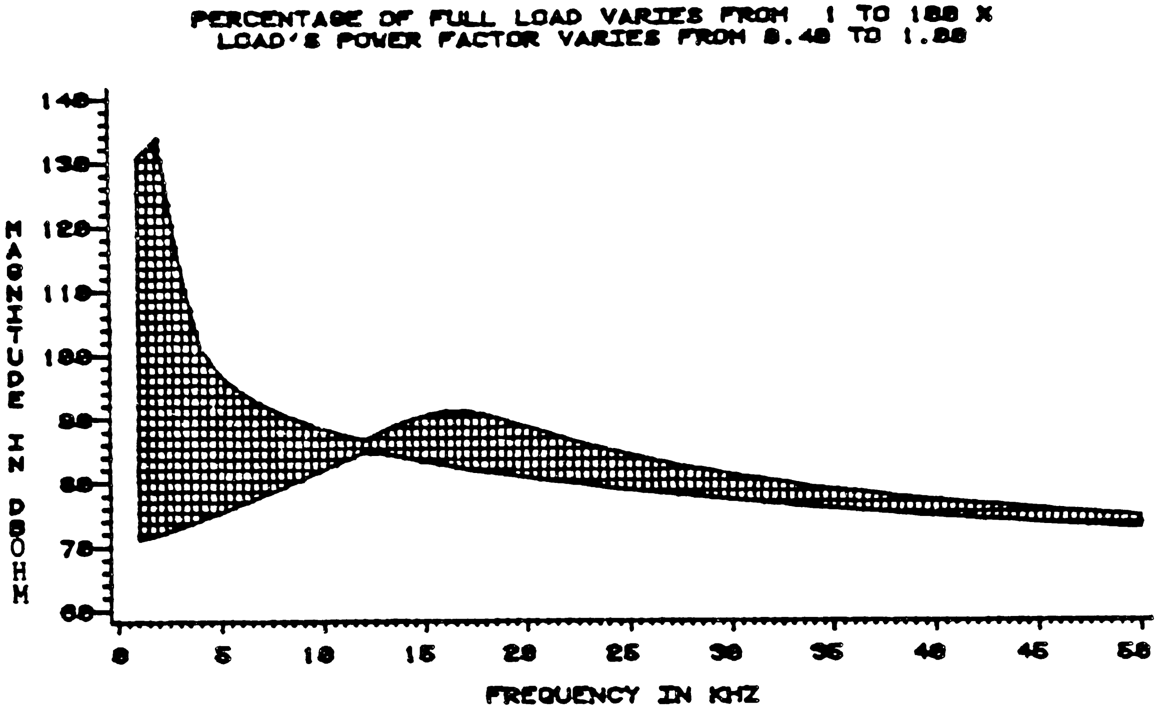

Figure 2.17 - Primary impedance magnitude range for a 50-KVA transformer

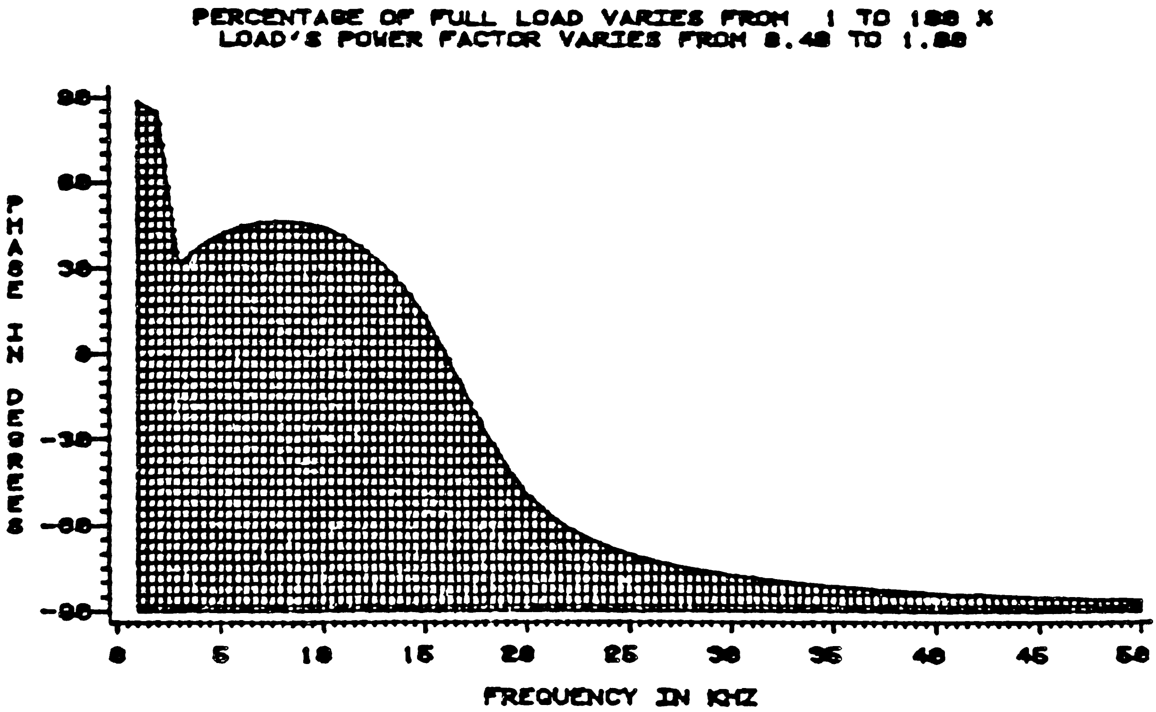

Figure 2.18 - Primary impedance phase range for a 50-KVA transformer

impedance being greater than 10 kilohms for frequencies up to at least 30-kHz.

Figure 2.14 shows the possible range of values of the phase angle of the primary impedance. As with the magnitude, a larger range is found at the lower frequencies. Below 4 or 5 - kHz this modeling technique yields almost no information since the phase angle is virtually unrestricted. The general shape of this phase range predicts a phase peak around 5-kHz for the 10 - KVA transformer. Once above this point of resonance, the impedance can be expected to be capacitive in nature. Furthermore, the resistive part of the impedance diminishes rapidly out to 20-kHz, where the impedance is almost purely capacitive.

Figures 2.15 to 2.18 contain the magnitude and phase ranges for 25 and 50-KVA transformers, respectively. These ranges are very similiar to the 10 - KVA transformer impedance ranges just discussed. A couple of trends should be noted, however. The possible impedance phase range increases slightly with increase in transformer size. Secondly, the phase and magnitude peaks shift slightly upward in frequency as transformer size increases. The magnitude of the primary impedance decreases very slightly with increasing transformer size, but still remains above 10 kilohms in almost all circumstances.

Several conclusions can now be drawn concerning the primary impedance of transformers for a generalized secondary load, based on the RLC plus ideal transformer model presented. Although the primary impedance of distribution transformers changes somewhat with transformer size and secondary load, the primary impedance still remains quite large. A good rule of thumb appears to be that the impedance will almost always be 10 kilohms or more, and decreases with frequency. A somewhat less restrictive generalization must be made for the phase of the primary impedance. Although the impedance is primarily capacitive in nature, care must be taken when considering frequencies below 10-kHz. For frequencies between 4 and 15 kHz, the impedance falls in the range where the phase peak occurs. It is therefore important that generalizations not be made for this range. Below about 4-kHz, this model does not provide enough conclusive evidence to draw any substantial conclusions about the phase of the impedance.

Consider now how the propagation parameters of interest change as a function of the transformer spacing. Because the transformer's primary impedance is capacitive at frequencies of interest, the addition of transformers to the distribution line simply adds additional capacitance to the line's characteristics. Increasing the number of transformers per mile therefore lowers the characteristic impedance and velocity of propagation without significantly effecting carrier signal attenuation.

Understanding the magnitude and phase of a distribution transformer's primary impedance is important in order to make effective use of the distributed model of a distribution line with associated transformers. Although it is possible to make further simplifications to equation 2.20 for certain circumstances, this task is left to the reader to suit his particular case. It is suggested that complete measurements be made of transformer primary impedance when one is concerned with a particular frequency.

3. Distribution Line Measurements

The next and probably most important step is the measurement and documentation of signal propagation along a power distribution line. Several problems arise in developing a measurement procedure that is both practical and provides meaningful results. Because of the many changing aspects of an actual distribution line, significant results can only be obtained by developing a very controlled test environment.

The recent completion of Carolina Power and Light Company's Distribution Test Facility near Raleigh, N.C. provided the necessary controlled environment. A four-mile section of single-phase overhead line was isolated from the rest of the Test Facility for these measurements. This section of line was initially setup with no transformers, loads, capacitor banks, etc. connected. Measurements could then be made to show the propagation effects of just the distribution line itself at DLC frequencies. Although no loads or other distribution equipment was attached to this distribution test line, the line was constructed according to the same standards specified for a distribution feeder providing power to customers. The importance of this is that the distribution test site is more than a mock up of a distribution line, it is an actual unloaded distribution line. After measurements had been made on the line by itself, twenty-four distribution transformers were connected to the line at a fairly equal spacing. The measurements were then repeated, yielding a complete before and after documentation of the effects of the transformers on the carrier signal propagation.

Two measurements were performed (each with and without the transformers in place). An FFT analyzer was used to document the input to output transfer characteristics for frequencies from 1 to 50-kHz. This procedure was also used to determine values for the characteristic impedance and attenuation constant. The second measurement was geared towards documenting the magnitude change in the voltage and current waveforms with distance along the line. The resulting data were then used to accurately establish carrier signal propagation on an unbranched, single-phase, overhead distribution line with and without distribution transformers.

3.1 Distribution Test Site

Carolina Power and Light Company's Distribution Test Site is an unloaded power distribution feeder in a controlled environment. Twenty – three kV (line – to – line voltage) single and three-phase lines in both overhead and underground configurations are available. An important feature is the ability to add and remove different length loops to alter the total length of line in use. Figure 3.1 shows an plan view of the physical layout of the test facility. In Figure 3.1 (and also Figure 3.2) every intersection of two line segments represents a pole location, while every line segment itself represents a section of overhead line and an underground line buried directly below. The Test Facility is constructed in a grid pattern, resulting in the line crossing over itself in some places at either 45 or 90 degrees.

A 20,847 ft. section of single-phase overhead line was isolated from the rest of the distribution test site for these measurements. Both ends of this section were disconnected by 200-amp primary oil switches (such as those used to switch capacitor banks). With the exception of these switches, the isolated section of distribution line was completely unloaded. The isolated single – phase overhead section of line is shown in Figure 3.2, and this section will be the object of investigation throughout the

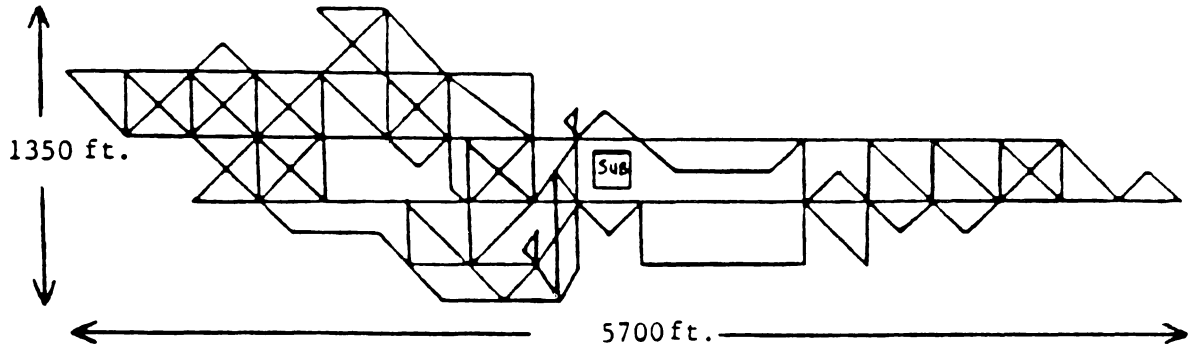

Figure 3.1 - Carolina Power and Light Company's distribution test site

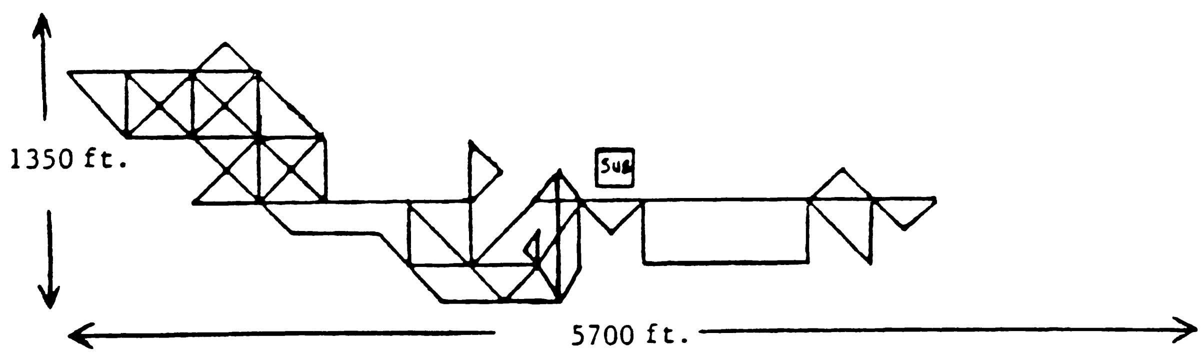

Figure 3.2 - Single-phase overhead section of the distribution test site

rest of this paper. Several construction characteristics of the line are relevant to the measurements and are mentioned at this point. The phase and neutral conductors are both #2 AWG aluminum which have a diameter of .2576 inches [9]. The height of the phase conductor varies from 25 to 50 ft. above ground, with the neutral conductor spaced 3 to 10 ft. below the phase conductor. The neutral conductor is earth grounded at every pole with bare copper (either #4 or #6 AWG). Although the distribution test site is constructed to be energized at 23-kV (line-to-line voltage), the test site was not energized with 60-Hz power during any of these measurements.

3.2 Voltage Transfer Characteristics

The first set of measurements was concerned with the voltage transfer characteristics of the test section in the frequency domain. These measurements are made in the frequency domain to obtain results at all frequencies of interest. A Nicolet-660B FFT analyzer was used in these measurements. The Nicolet-660B is a two-channel instrument capable of computing a transfer function using one channel as the input, and the second channel as the output. For a complete description of the Nicolet – 660B, the interested reader is referred to reference [15] or the Nicolet operating manual. One of the options provided on the Nicolet 660B is a random noise source that provides an input that is flat (in the frequency domain) up to 100-kHz. A diagram of the measurement equipment setup is shown in figure 3.3.

The distribution line shown in figure 3.3 is the 20,847 ft. single – phase overhead test section mentioned previously. Each end of this test section is connected to the measurement equipment by a 60-ft. length of 16 gauge, twisted wire pair. These 60-ft. lengths are physically clamped onto the phase and neutral conductors to obtain a good metallic contact. The amplifier shown in figure 3.3 is a Harmon/Kardon, Citation-sixteen model. Amplification of the random noise input signal was necessary to obtain an

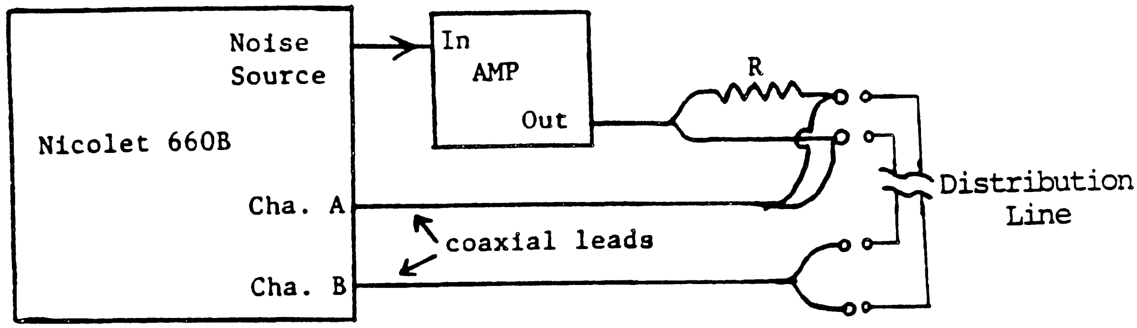

Figure 3.3 - Transfer function measurement equipment setup

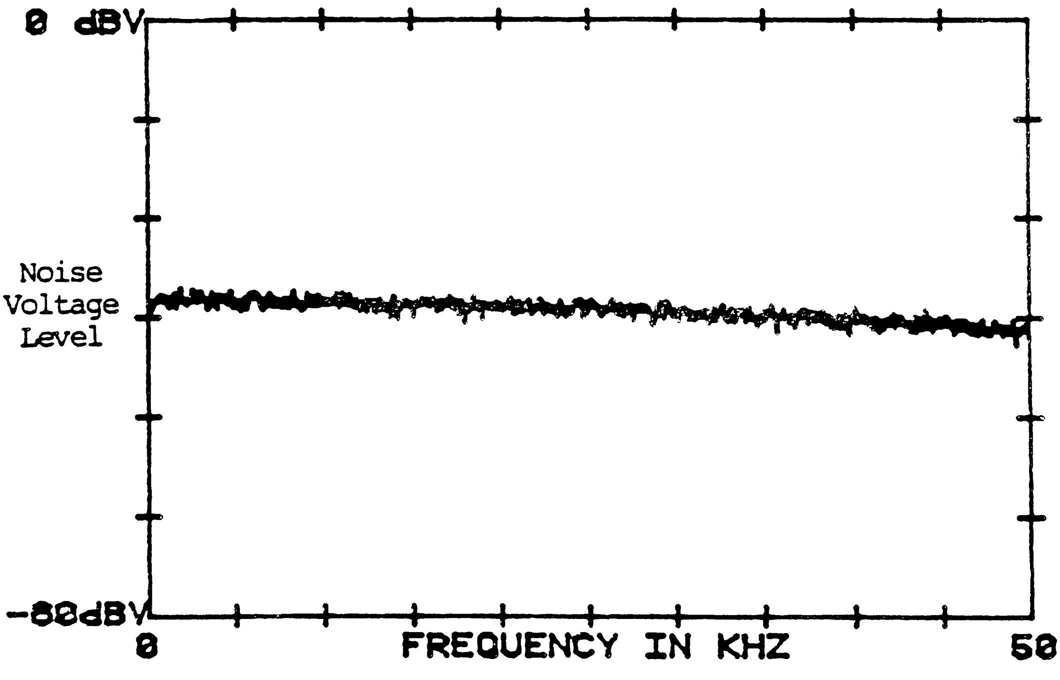

Figure 3.4 - Output of the random noise source after amplification

output signal sufficiently strong throughout the entire band of interest. The output of the amplifier is shown in figure 3.4 with the random noise source as it's input. A series impedance matching resistor was inserted between the amplifier and the input end of the test line. Channel A of the Nicolet was also connected to the input end of the test line. The other end of the test line was then connected to channel B of the Nicolet. For reference purposes, one physical end of the test section is defined as the beginning of the line, or the input point. The other end of the test section is defined as the end of the line, or the output point.

Both channels of the Nicolet have an input impedance of 100 kilohms, and therefore present essentially open circuits to the line. The magnitude response of the transfer function (output divided by input) is shown in figure 3.5 for 0 to 50-kHz.

Before any conclusions are drawn, it is first essential to understand what causes the pattern of figure 3.5. The resonant peaks shown in figure 3.5 are the result of the reflection caused by the open circuit at the end of the line (the 100 kilohm impedance presented by the Nicolet). This reflection results in a standing-wave pattern on the line. It is known that a voltage maximum, or anti-node, will always occur at the end of line if that end of the line is open-circuited. Another property of a standing-wave is that the distance between two voltage nodes is a half-wavelength (a voltage node being a local minimum [1,4,13]. Furthermore, the voltage nodes are equally spaced with respect to the voltage anti-nodes such that the nodes and anti-nodes are one quarter-wavelength apart.

Consider now what information is contained in figure 3.5. Each point on the curve represents the magnitude response of the voltage at the end of the line to the beginning of the line (output over input). The voltage is always a maximum at the output (because of the open circuit), whereas the voltage at the input changes with frequency. The magnitude of this transfer function should therefore be at it's maximum value when the voltage at the input is a minimum. Furthermore, the voltage at the input is a maximum when the input is a quarter-wavelength, three quarter-wavelengths, etc., from the end of the line. The lowest frequency peak in figure 3.5 therefore corresponds to the frequency at which the physical length of the line is equal to the electrical quarter-wavelength.

Several very important conclusions can now be drawn from figure 3.5. First of all, the magnitude of the transfer function returns to 0 dB at it's minimum points. These minimum points correspond to the frequencies where

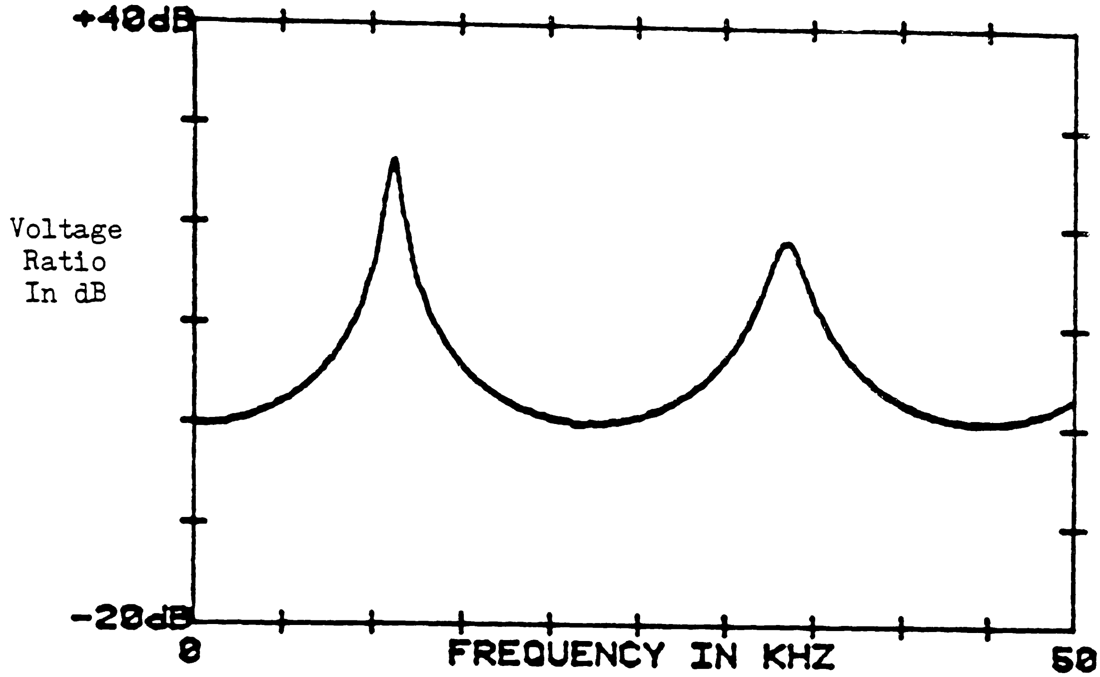

Figure 3.5 - Voltage-ratio of the distribution line terminated in an open-circuit

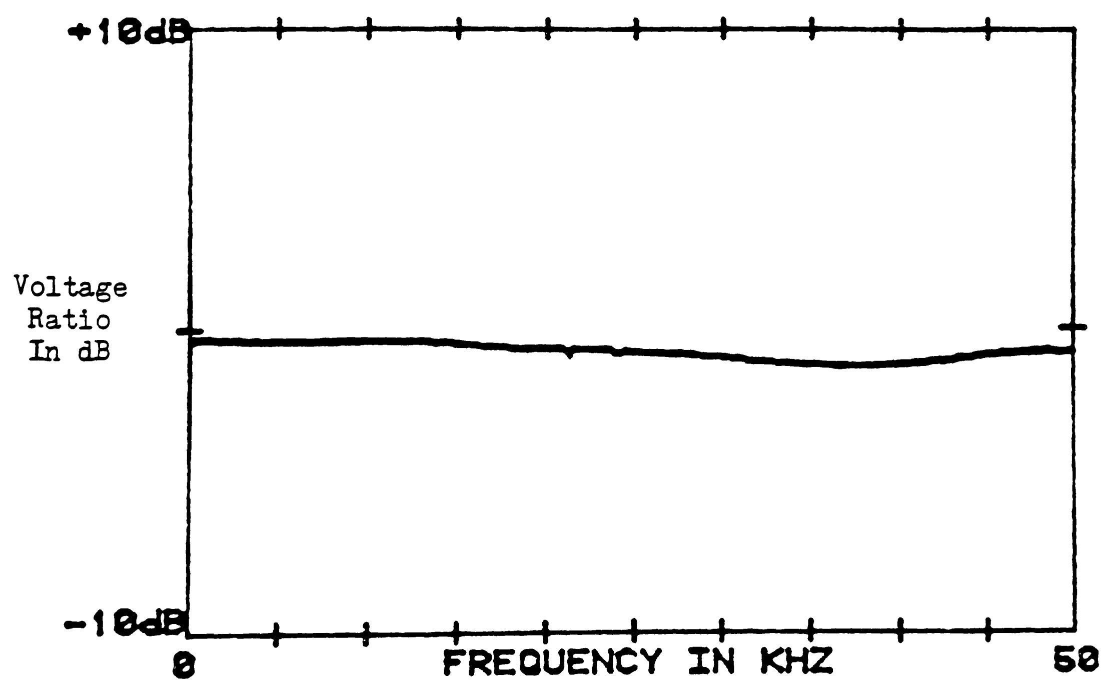

Figure 3.6 - Voltage-ratio of the distribution line terminated in 450 ohms

the line is electrically a half-wavelength and one wavelength long. At these points, the voltage waves add in phase, just as they do at the end of the line. Therefore, a 0 dB change from input to output at these frequencies implies that there is very little loss on the line itself. This will be discussed in greater detail after the presentation of additional results. A second result concerns the propagation velocity of the wave on the distribution line. From figure 3.5, the line is an electrical quarter-wavelength long at a frequency of 11.250 kHz. The physical length of this distribution line has been measured at 20,847 ft., accurate to within 1 percent. The velocity of propagation can be calculated from these quantities according to

$$V_p = \lambda f \tag{3.1}$$

This results in a velocity of propagation of 177,673 miles per second. When compared with the speed of light in air [8], the velocity of propagation along an unloaded power distribution line is 95.4 percent of the speed of light. This important result documents the conclusion that the velocity of propagation is not equal to the speed of light in air, as one might initially expect, but is instead approximately 5 percent less. Finally, as now expected, the second peak of figure 3.5 occurs at the frequency where the physical line length is equal to three-quarters of the wavelength.

This simple measurement technique provides a very powerful tool for documenting carrier signal propagation on distribution lines. Several measurements were made using this procedure to provide a basic research foundation for the design of DLC systems. As a first step, the termination at the end of the line was changed to a variable resistor to enable measurement of the characteristic impedance. Once a value for Zo was established, the line's loss and phase shift characteristics could be determined. The final measurements using this procedure were made after 24 distribution transformers were attached to the distribution line, enabling an excellent before and after presentation.

One fact well documented by all texts on transmission line theory is that the reflections caused by standing waves are eliminated when the transmission line is terminated into an impedance equal to the line's characteristic impedance [1,4,8]. In order to determine the characteristic impedance of the distribution line, the end of the line was terminated in a variable resistor (i.e., in parallel with the 100 kilohm input impedance of the Nicolet). This resistance was then adjusted until the pattern of figure 3.5 was "flattened" as much as possible.

For the completely unloaded line, a resistance of 453 ohms was the most effective in eliminating the standing-wave. With this termination, measurement of the magnitude of the transfer function resulted in figure 3.6. For frequencies up to 50-kHz, the loss is less than 1 dB, or .25 dB per mile. It is apparent that the distribution line itself can be considered as a almost lossless medium at these frequencies.

Although the characteristic impedance was measured at 453 ohms, the reflection caused by a small variation in the terminating impedance around this value was insignificant. As much as a 5 percent change in the terminating impedance resulted in virtually the same pattern as figure 3.6.

The phase component of the transfer function with a 453 ohm termination is shown in figure 3.7. Note that this graph is modulo 360 degrees from 180 to -180 degrees, resulting in the discontinuous jump from -180 to 180 degrees near the middle of the graph. Knowing the line length to be 20,847 ft., we now know the phase shift per unit distance for frequencies up to 50-kHz. For example, at 45-kHz, the phase shift is -360 degrees, or -91.2 degrees per mile. Furthermore, figure 3.7 shows that the line's phase shift is linear with frequency.

As the final step in this measurement procedure, 24

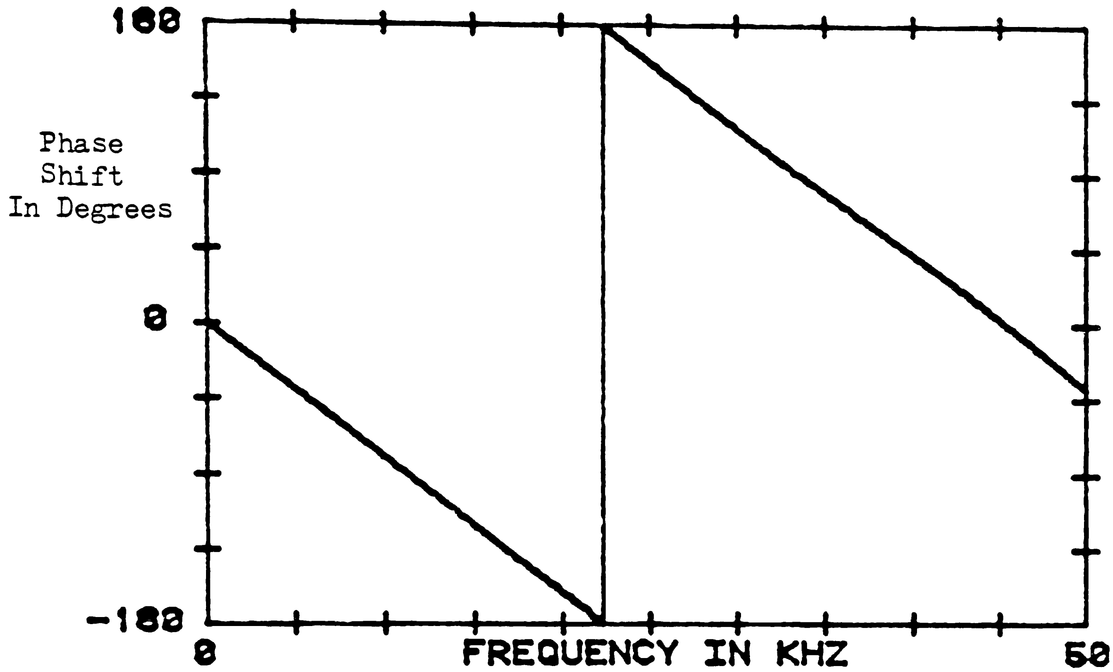

Figure 3.7 - Phase-shift of the distribution line terminated in 450 ohms

distribution transformers were attached to the distribution line. All were 25-KVA transformers. The previous measurements were repeated with the secondaries of the transformers both open and short-circuited. Figures 3.8 and 3.9 are the magnitude of the transfer function with the end of the line terminated in an open-circuit and the transformer's secondaries open and short-circuited, respectively. Figures 3.10 and 3.11 are the same as 3.8 and 3.9, only the end of the line is now terminated into it's respective characteristic impedance (a new value). With the

transformer's secondaries open-circuited (figure 3.10),

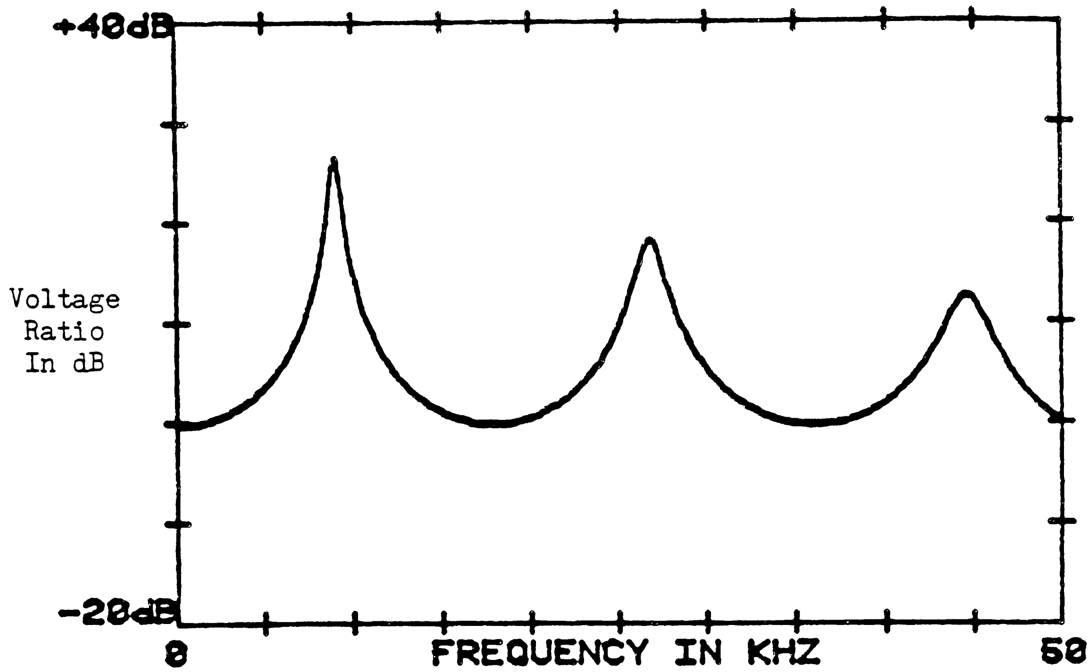

Figure 3.8 - Voltage-ratio of the distribution line with transformers, secondaries open-circuited, line terminated in an open circuit

this new characteristic impedance is 381 ohms. With the secondaries short – circuited (figure 3.11), the characteristic impedance was lowered even further to 358 ohms. Finally, the phase components of the transfer function with the end of the line terminated in it's respective characteristic impedance are shown in figures 3.12 and 3.13. Figure 3.12 is with the transformer's secondaries open-circuited, and figure 3.13 is with the secondaries short-circuited.

In analyzing the results, first consider the effects of the transformers on the magnitude of the transfer function as shown in figures 3.8 and 3.9. Although the

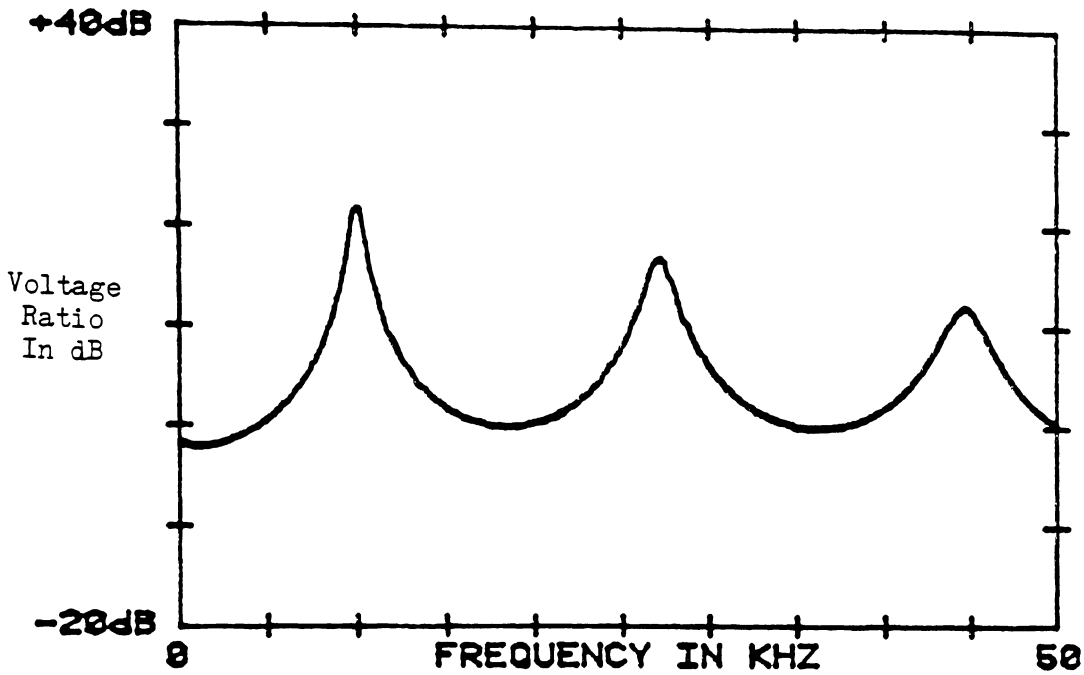

Figure 3.9 - Voltage-ratio of the distribution line with transformers, secondaries short-circuited, line terminated in an open circuit

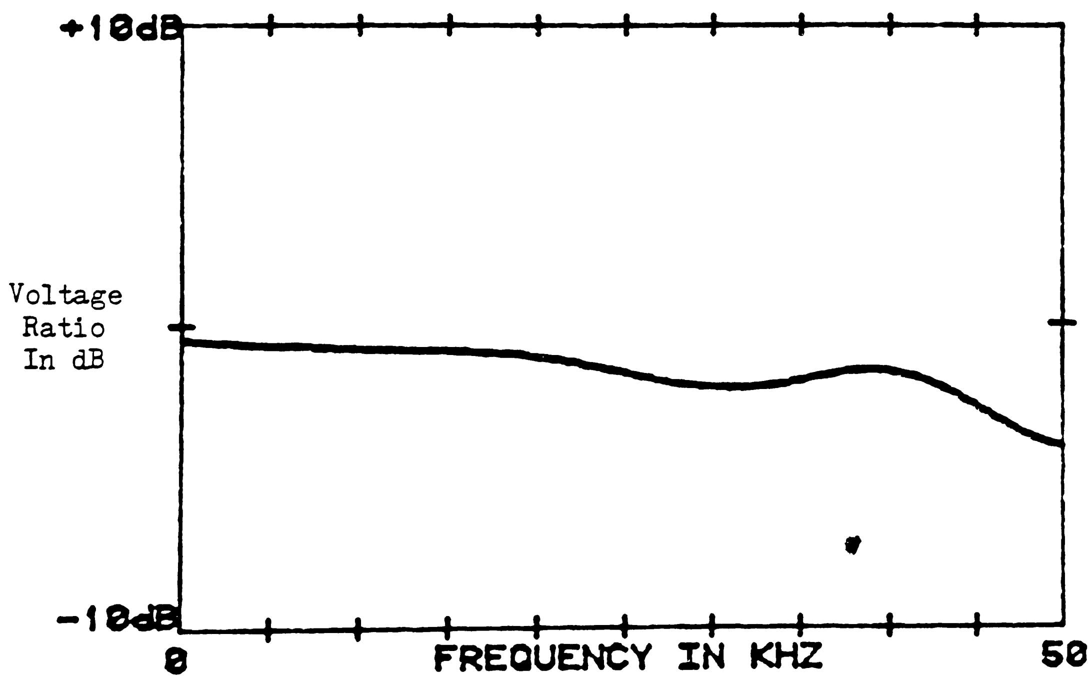

Figure 3.10 - Voltage-ratio of the distribution line with transformers, secondaries open-circuited, line terminated in 364 ohms

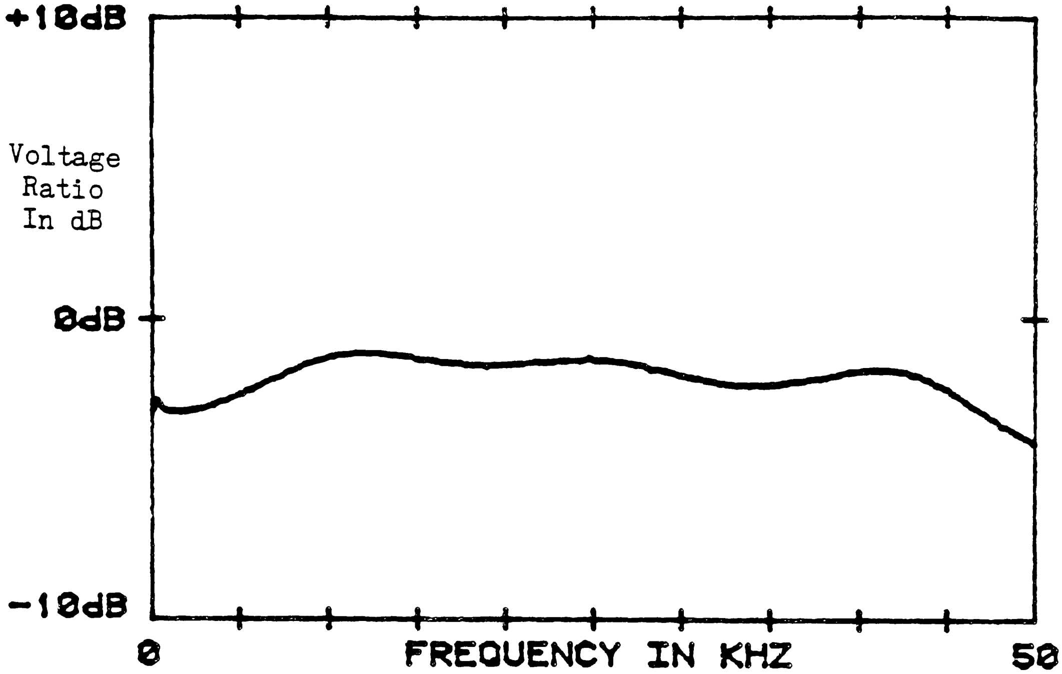

Figure 3.11 - Voltage-ratio of the distribution line with transformers, secondaries short-circuited, line terminated in 381 ohms

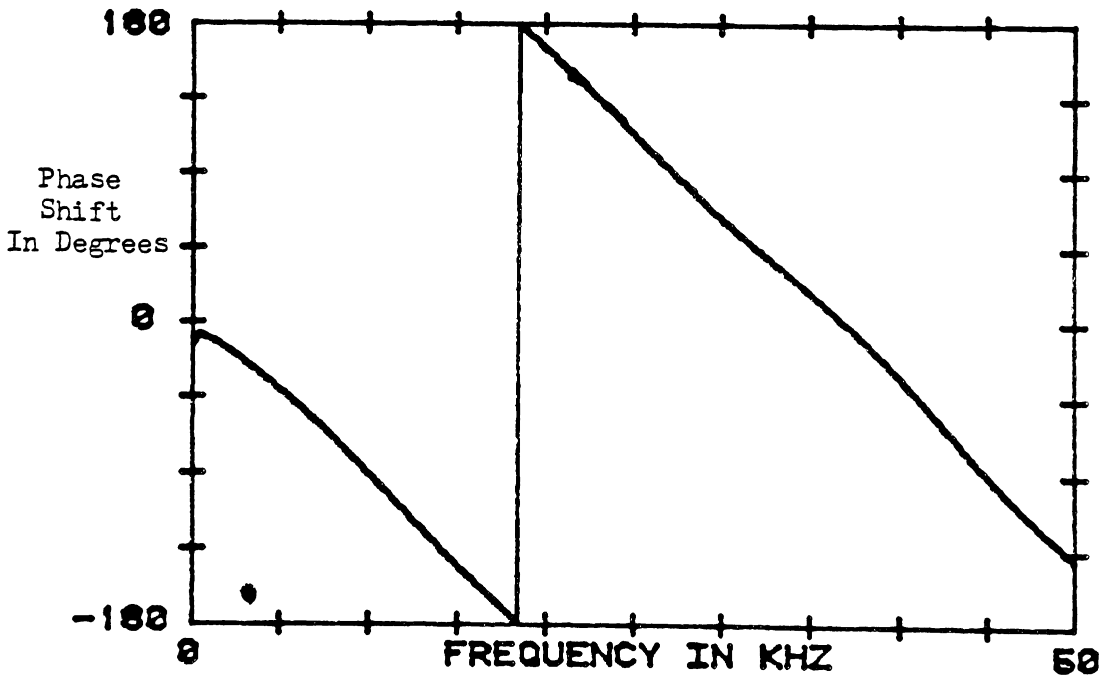

Figure 3.12 - Phase-shift of the distribution line with transformers, secondaries open-circuited, line terminated in 364 ohms

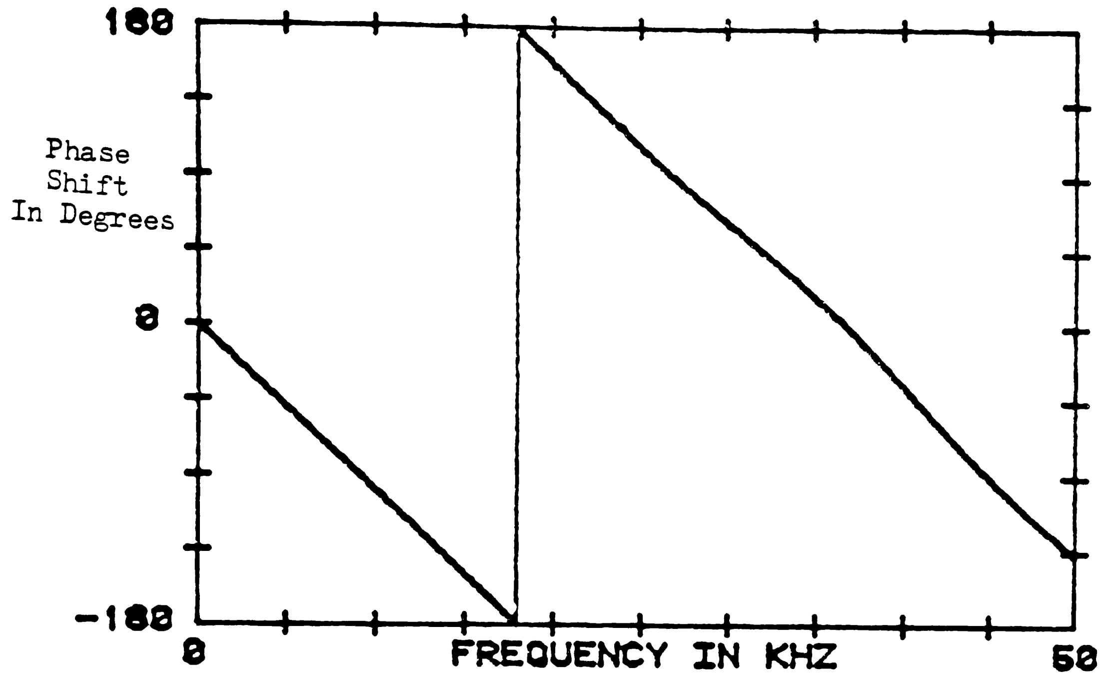

Figure 3.13 - Phase-shift of the distribution line with transformers, secondaries short-circuited, line terminated in 381 ohms

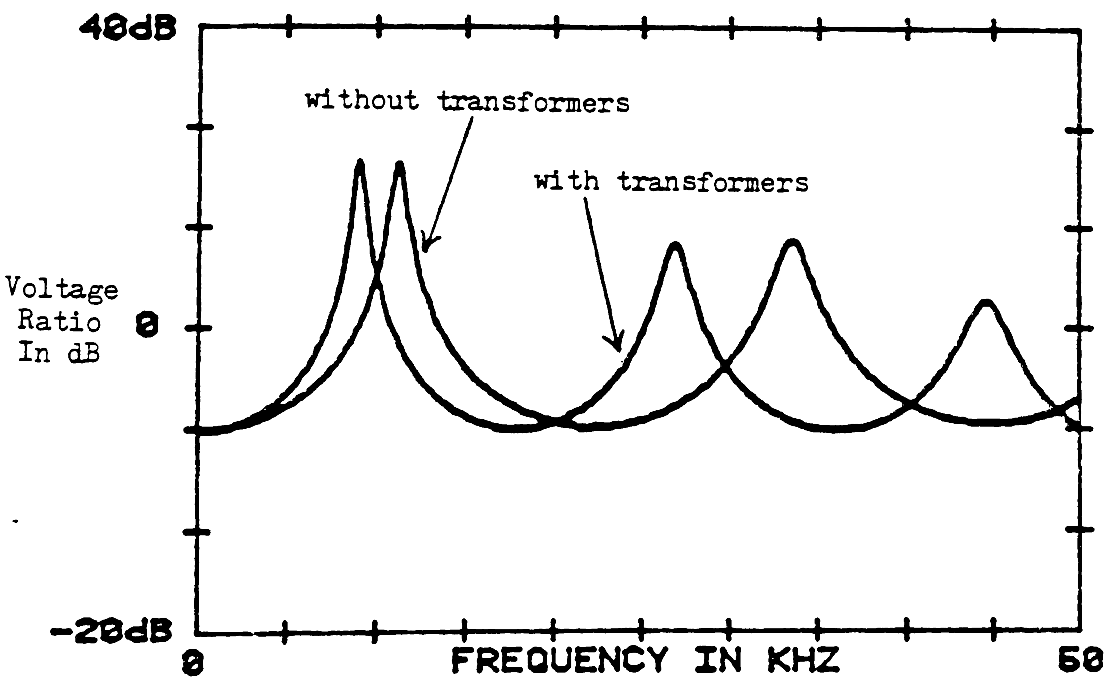

Figure 3.14 - Voltage-ratio of the distribution line with and without transformers, line terminated in an open-circuit

relative levels of the peaks and valleys have not changed, they have been shifted down in frequency significantly. Figures 3.5 and 3.8 are shown overlapped in figure 3.14 for a clearer comparison. On the other hand, the secondary load (i.e., either an open or short-circuit) has very little impact. Comparing figures 3.8 and 3.9, the first peak is just slightly higher and at a lower frequency when the transformers are unloaded (secondaries open-circuited) than when they are fully loaded (short-circuited). For frequencies greater than 15-kHz, figures 3.8 and 3.9 are essentially identical, and we may conclude that the secondary load has little impact. The effect of the distribution transformers on the magnitude of the transfer function may be generalized as follows. With the physical length of the line remaining constant, the addition of the transformers has resulted in the distribution line appearing electrically longer. This may be viewed in several ways. One is that the velocity of propagation along the line has been reduced. With the secondaries of the transformers short-circuited, the first peak occurs at 10.0-kHz (see figure 3.9). This corresponds to a velocity of propagation of 157,932 miles/sec, or 84.8 percent of the speed of light. Alternatively, and perhaps better, the relative permitivity of the distribution line has been increased, therefore increasing the capacitance of the line. This point of view agrees well with the assumption that the primary impedance of distribution transformers would be capacitive at DLC frequencies. Without further comment on this topic at this point, consider now the change in the characteristic impedance.

There are two points of interest. The addition of the 24 transformers reduced Zo from around 450 ohms to between 350 and 380 ohms depending on the secondary loading of the transformers. Zo is lowest when the transformers are present, but lightly loaded. Secondly, the resistive termination was not as successful in completely eliminately the standing-wave pattern. One possible explanation for this is that with the addition of the transformers, Zo may no longer be purely resistive, and the reactive part of the characteristic impedance may become important.

Previously, it was shown that the single-phase, overhead distribution line by itself was essentially a lossless medium at DLC frequencies. It now remains to show how the attenuation changes with the addition of distribution transformers. Consider figures 3.10 and 3.11. Although the graphs in these figures are not as smooth as that of figure 3.6, the input to output loss is never greater than 3 or 4 dB for frequencies below 50-kHz. Furthermore, from 5 to 25-kHz, the most popular range for current DLC systems, the loss is less than 2 dB. This corresponds to approximately .5 dB per mile. Although this loss is small, it should not be completely ignored, especially for long distribution feeder runs. It is very important to note that the maximum per mile line loss increased from .25 to .5 dB with the addition of 24 transformers over 20,847 ft., or 6.1 transformers per mile. This result is a good indication of the effect that distribution transformers have on signal attenuation.

Only a small change in the phase of the transfer function resulted with the addition of the transformers. The phase shift is still linear with frequency (although a very slight curvature is detectable when the transformer's secondaries are short-circuited). However, the magnitude of the phase shift per unit distance has increased by around 20 percent.

3.3 Signal Propagation vs. Distance Measurements

This second set of signal propagation measurements is aimed at documenting the actual magnitudes of the voltage and current waveforms as they propagate along the previously described test section of distribution line. The basic procedure is to inject a carrier signal onto the beginning of the test section, and then to measure the magnitude of the voltage and current waveforms at many points along the line. In the past, such a measurement procedure was unrealistic because of the lack of a controlled test environment and the obvious safety problems.

The transmitting equipment was setup is shown in figure 3.15. The input amplifier has a low output impedance of about 2 ohms. For this reason, a series resistor was used to match the impedance to the line's characteristic impedance (which was determined in section 3.2). Although this measurement was made with three different terminations at the end of the line (open circuit, short-circuit, and characteristic impedance), only the results with an open-circuit and characteristic impedance termination are presented in this paper. A transmission frequency of 25-kHz was chosen to satisfy two requirements. It was desired that the frequency be high enough that at least one voltage node and anti-node were

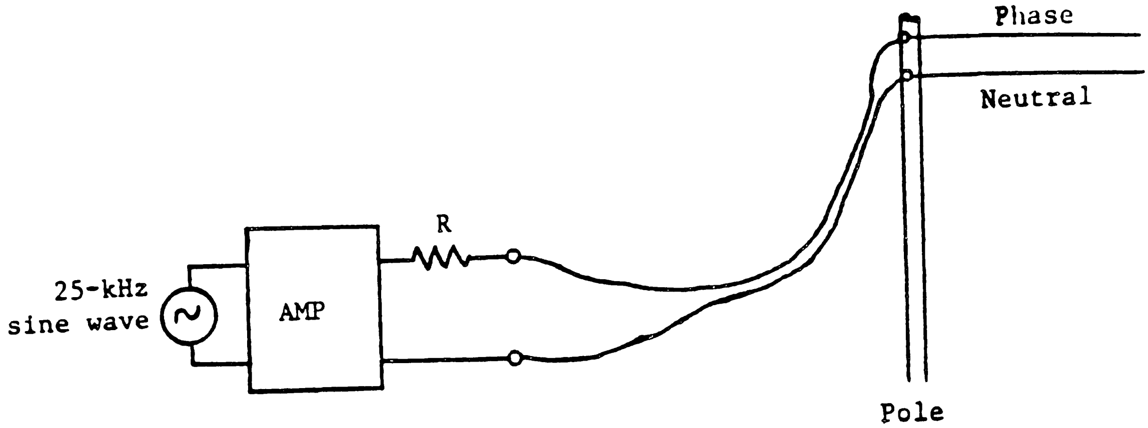

Figure 3.15 - 25-kHz carrier injection equipment setup

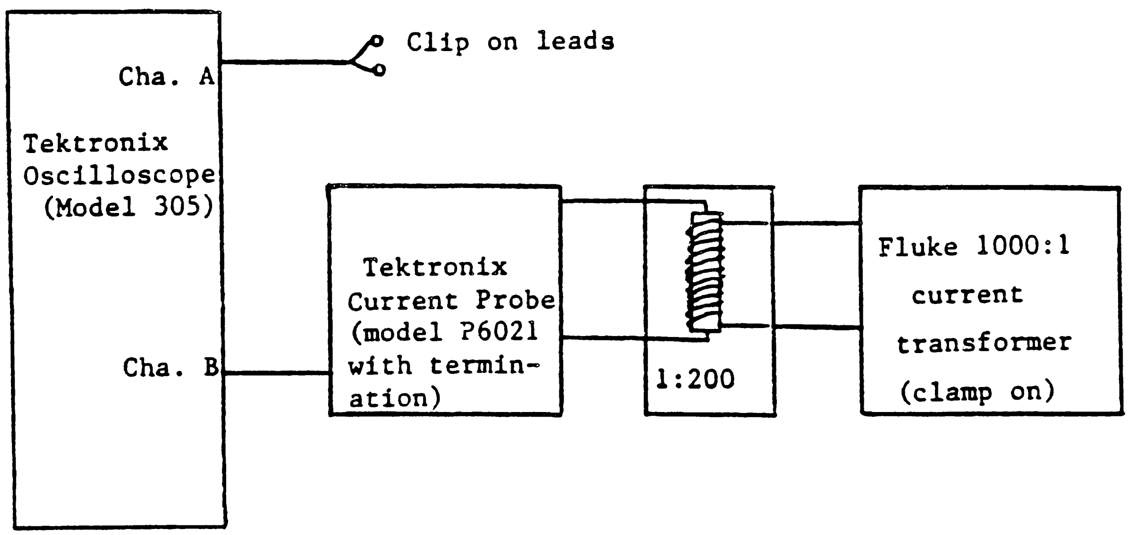

Figure 3.16 - Portable measurement equipment setup

present on the 20,847 ft. distribution line. On the other hand, it was desired that the frequency be as close as possible to the frequency range used by current DLC systems. The magnitude and frequency of the input signal was constantly regulated during the measurement procedure.

The actual measurement of the magnitude of the voltage and current waveforms was accomplished through the use of a portable oscilloscope (Tektronix model 305 dmm) in a bucket truck. Both of the oscilloscope's inputs are high impedance (i.e., 1 Megohm), and one input was used to measure the voltage from the phase wire to the neutral wire with a direct, clip-on connection. The current waveform was measured using a combination of two current probes. A diagram of the measurement equipment is shown in figure 3.16. A Fluke clamp-on 1000:1 current transformer was clamped around the conductor in which the current was being measured. The secondary of this transformer was short circuited, providing a true current transformer that was independent of the impedance presented to the input. Since the transmission level was relatively low to start with, the output current of the Fluke probe had to be increased to compensate for the 1000:1 decrease. To accomplish this, 200 turns of the Fluke's secondary were placed on the primary side of a second current probe, a Tektronix P6021 with termination (matched for input to an oscilloscope).

The resulting input to output characteristics were then calibrated at 25 - kHz, for varying input currents and impedances. The overall input current to output voltage (displayed on the second channel of the oscilloscope) was found to be constant over all inputs of interest for this application, and this factor was then taken into account before converting the raw data into graphical form. While the measurements were being taken, a brief test was made to check for any interference between the voltage and current probes. No such interference was found.

Measurements were first taken on the 20,847 ft. section with only the transmitting equipment attached to the line. Approximately 40 measurement points were taken along this section. At each measurement point, the voltage from phase to neutral, the primary current, and the neutral current were measured. The characteristic impedance of the line was known to be 450 ohms, and this value was therefore used for the matching resistor at the input and the terminating resistor at the end of the line (when used). Plots of the voltage and current vs. distance from the end of the line are shown in figures 3.17 and 3.18, respectively. Additionally, the input impedance of the line and the neutral current (as a percentage of the primary current) are also shown in figures 3.19 and 3.20. As a matter of convenience, the x-axis in each of these

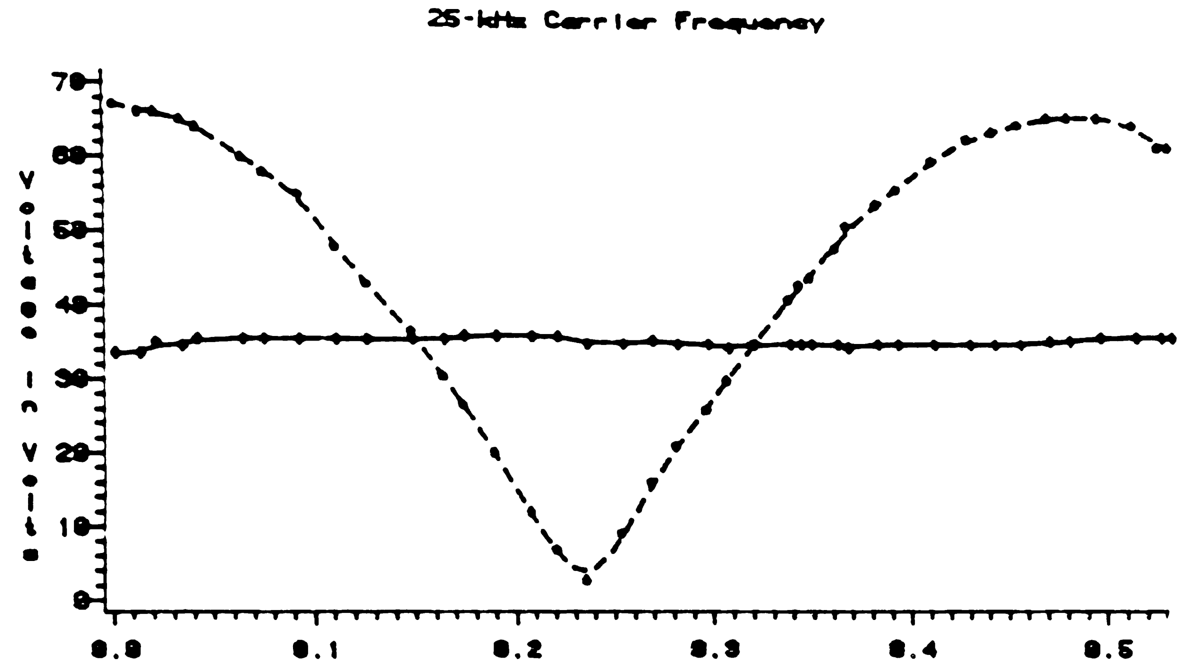

Fraction of Free-Space Wavelength From End of Line

LEGEND: TERM —◆— OC —◆— ZO

Figure 3.17 - Voltage magnitude vs. distance for the distribution line (free-space wavelength = 11.44 miles)

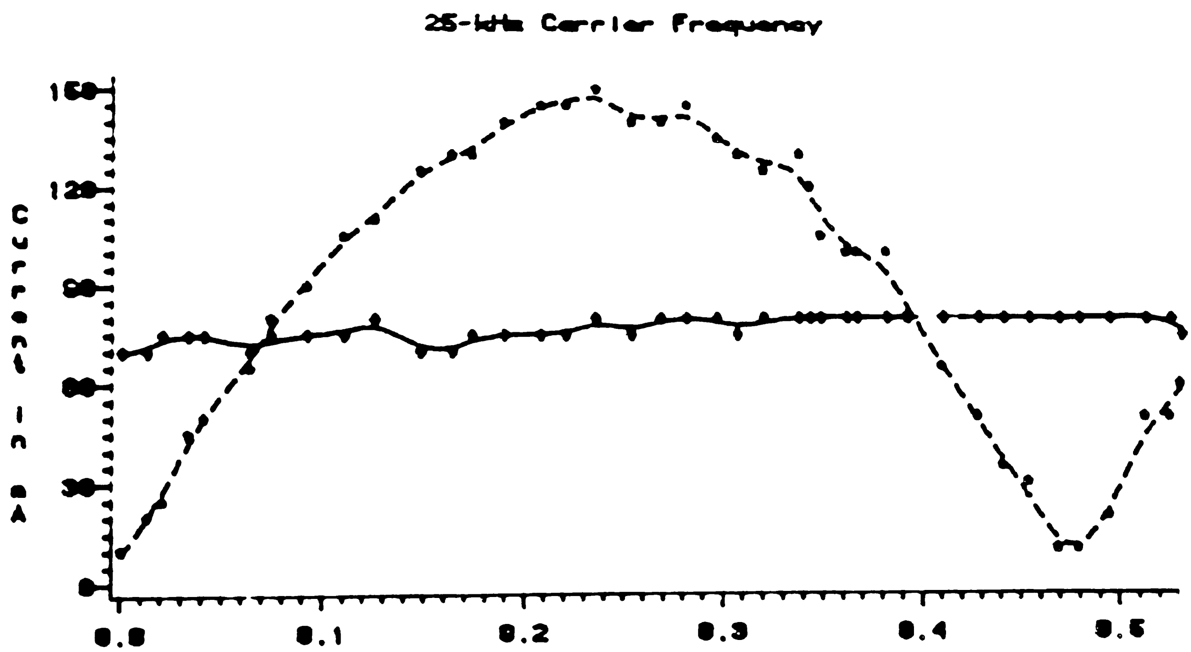

Fraction of Free-Space Wavelength From End of Line

LEGEND: TERM —◆— OC —◆— ZO

Figure 3.18 - Primary current magnitude vs. distance for the distribution line (free-space wavelength = 11.44 miles)

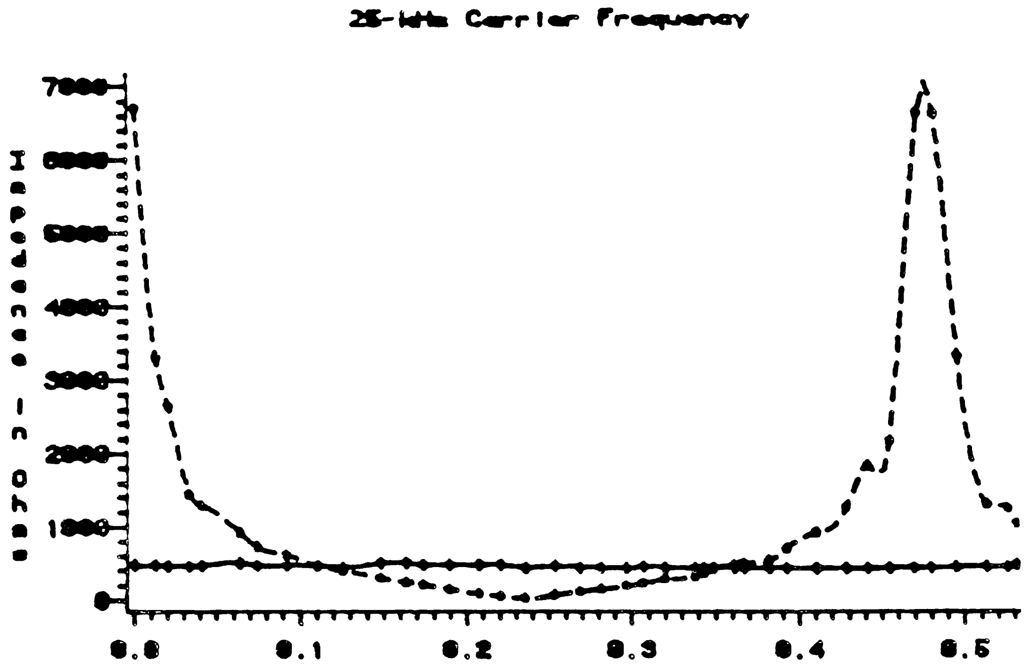

Fraction of Free-Space Wavelength From End of Line

LEGEND: TERM ◆-◆-◆ OC ◆—◆—◆ ZO

Figure 3.19 - Impedance magnitude vs. distance for the distribution line (free-space wavelength = 11.44 miles)

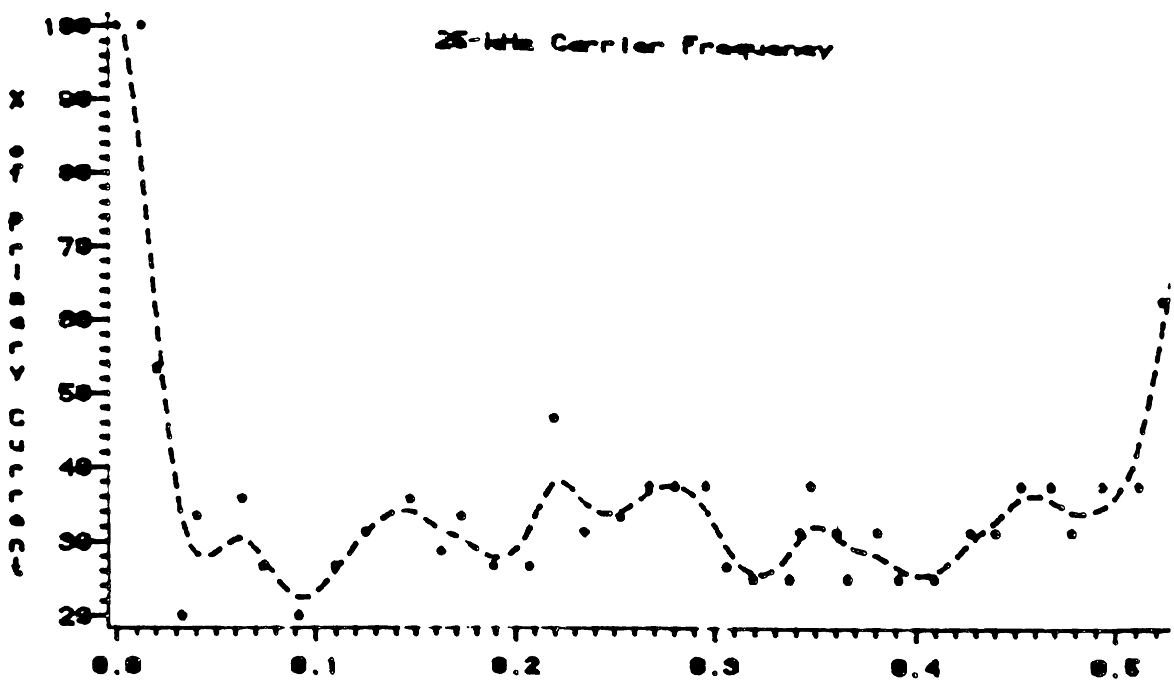

Fraction of Free-Space Wavelength From End of Line

End of line is terminated in Zo (450 ohms)

Figure 3.20 - Neutral current as a percentage of primary current for the distribution line (free-space wavelength = 11.44 miles)

plots has been converted to the distance in wavelengths (at 25 – kHz) from the end of the line. Each measurement point is shown on the plots, and then the points are connected using a spline function [10].

Consider first how the voltage changes with distance along the line, as shown in figure 3.17. As expected, a standing-wave pattern resulted when the line was terminated in an open circuit. The voltage standing-wave ratio (VSWR) is approximately 67/3.5 = 19.1, or 25.6 dB. This represents the worst case loss due to standing waves since the open-circuit termination causes a complete reflection and the line is essentially lossless. On the other hand, the VSWR is unity when the line is terminated into 450 ohms, the characteristic impedance of the line. Examining figure 3.18 shows very a similiar pattern for the primary current, except that the current and voltage are "opposite" in the sense that current nodes occur where voltage anti-nodes occur and vice-versa. A major point of interest is the location of these nodes. As shown in figure 3.17, with the line terminated in an open-circuit, the first voltage node occurs at approximately .236 wavelengths from the end of the line. This implies that the velocity of propagation is only 94.4 percent of the speed of light. An almost identical conclusion was reached in section 3.2 (95.4 was the number reached in that section). The conclusion that the velocity of propagation at DLC frequencies on an unloaded distribution line is approximately 95 percent of the speed of light is now the result of two different measurement techniques.

A well known characteristic of standing-wave patterns is that the nodes (minimum points) are sharply defined, whereas the anti-nodes (maximum points) have much broader peaks. This characteristic results in the impedance at points along the line having the pattern described in figure 3.19. This is especially important as it shows that at some points, the impedance of the line is quite high, as much as two orders of magnitude above it's average. Note that when the line is terminated into 450 ohms, the impedance of the line remains constant in the neighborhood of 450 to 470 ohms throughout the entire length of the line. Figure 3.20 shows one final important result. The current in the neutral wire is generally less than 40 percent of the current in the primary wire. This implies that 60 percent or more of the return path is through the earth's surface. The exact percentage generally varies with the type of soil and it's moisture content. The Distribution Test Site is located in a heavily wooded area near a lake, implying that a fairly high moisture content was present for these measurements. This area is slightly swampy and the soil also has a high content of clay in some parts.

These measurements were repeated after the twenty-four 25 - KVA distribution transformers were installed on the 20,847 ft. test section. The secondaries of all the transformers were short-circuited, as it was felt that this provided a closer approximation to a "normal" load, than an open - circuit would. A resistance of 380 ohms was used as the characteristic impedance termination for these measurements. Results from these measurements are probably the most important of this series as they are very similiar to actual distribution feeders in use. The change in the magnitude of the voltage and current with distance are shown in figures 3.21 and 3.22, respectively. The impedance and the neutral current (again as a percentage of primary current) are plotted in the same manner in figures 3.23 and 3.24.

Notice in figure 3.21 how the standing - wave pattern has shifted to the left, as compared with figure 3.17. The first voltage node now occurs at .205 wavelengths from the end of the line. This now implies that the velocity of propagation has decreased to 83.6 percent of the speed of light in air. This agrees with the 84.8 percent result obtained in section 3.2. As mentioned in that section, a better way of viewing this change is that the transformers add capacitance to the distribution line, therefore

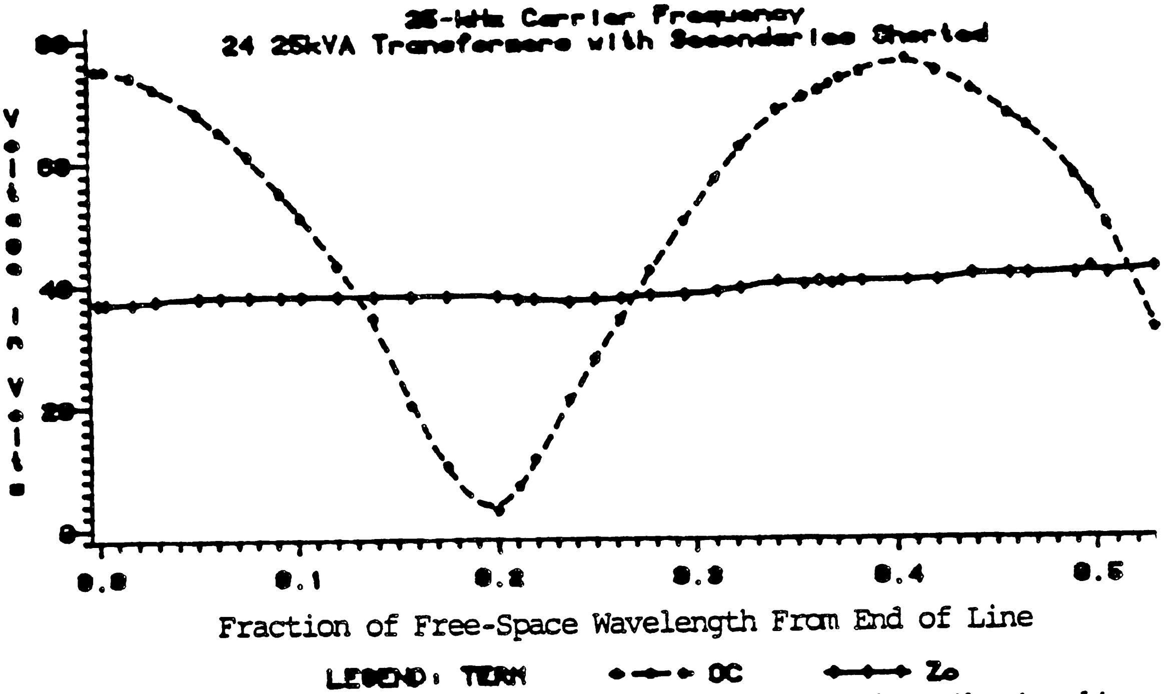

Figure 3.21 - Voltage magnitude vs. distance for the distribution line with transformers, secondaries short circuited (free-space wavelength = 11.44 miles)

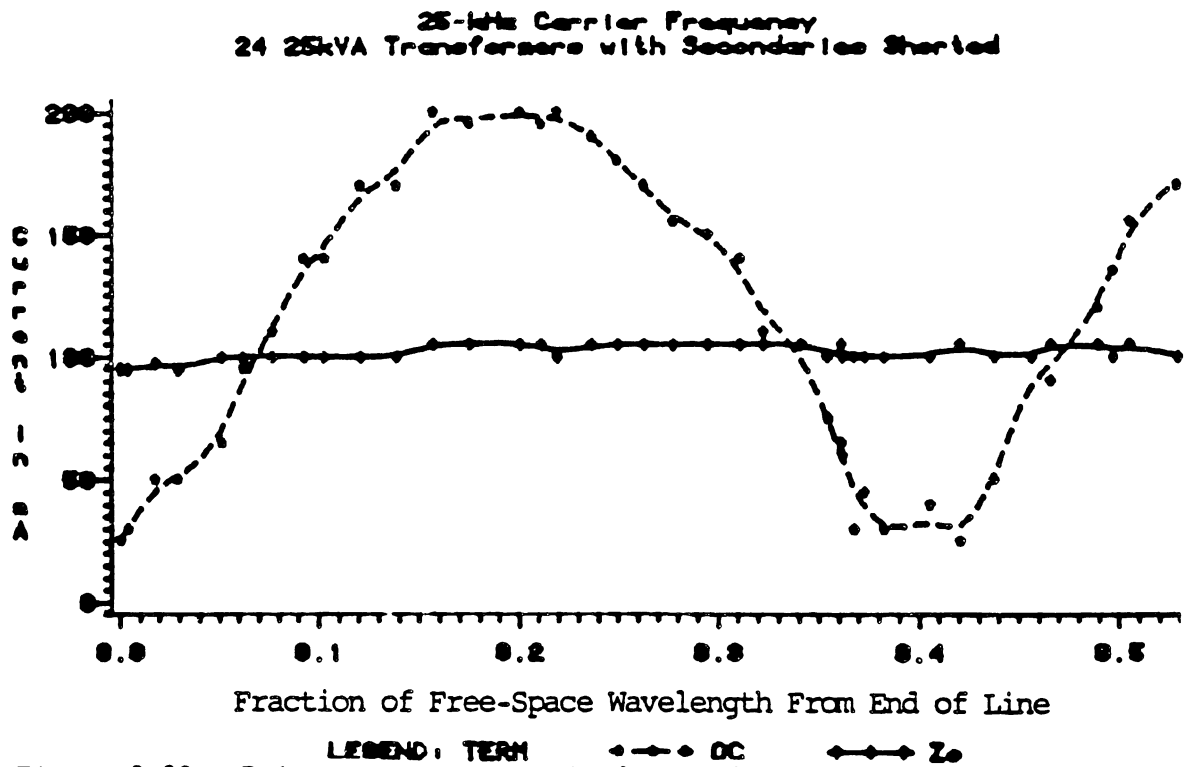

Figure 3.22 - Primary current magnitude vs. distance for the distribution line with transformers, secondaries short circuited (free-space wavelength = 11.44 miles)

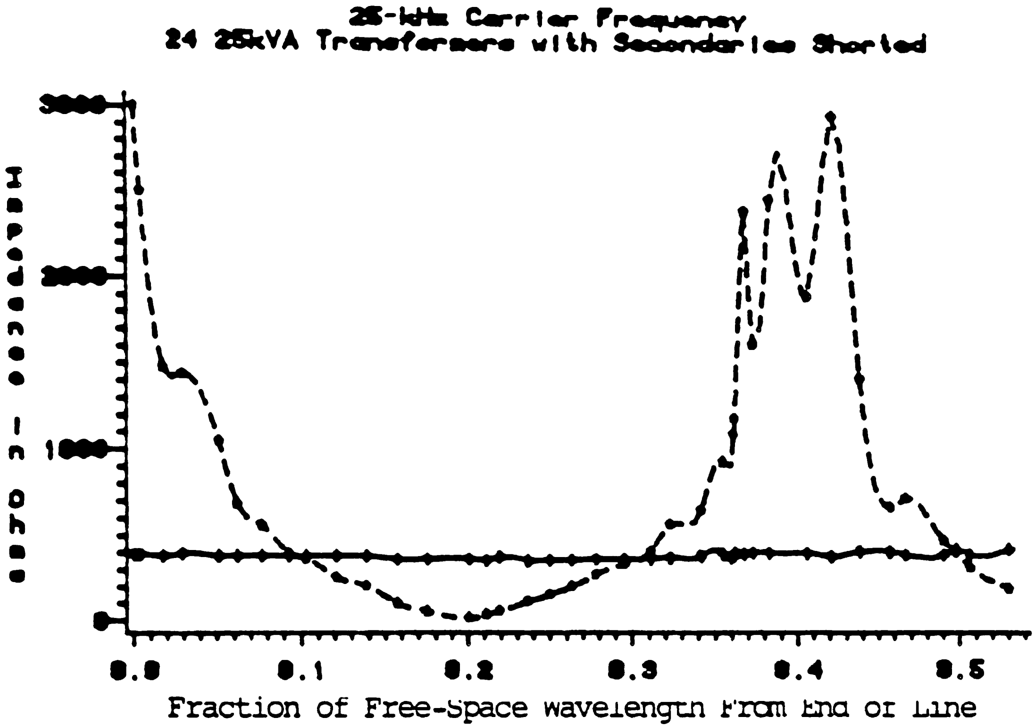

Figure 3.23 - Impedance magnitude vs. distance for the distribution line with transformers, secondaries short circuited (free-space wavelength = 11.44 miles)

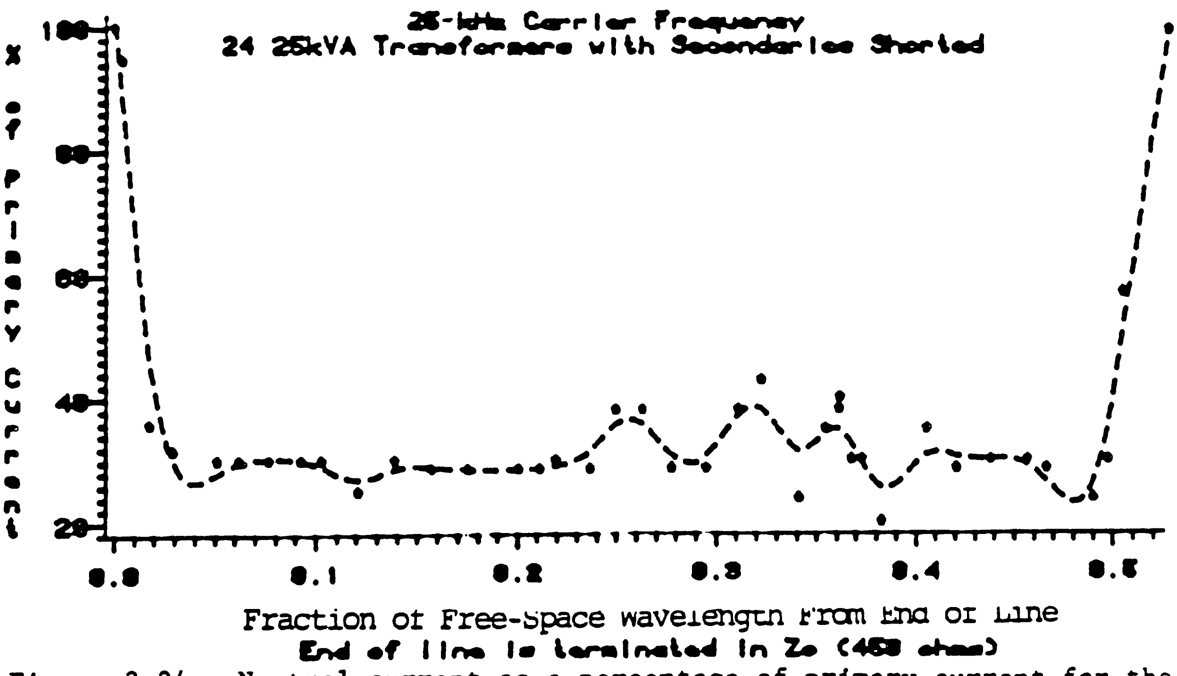

Figure 3.24 - Neutral current as a percentage of primary current for the distribution line with transformers, secondaries short circuited (free-space wavelength = 11.44 miles)

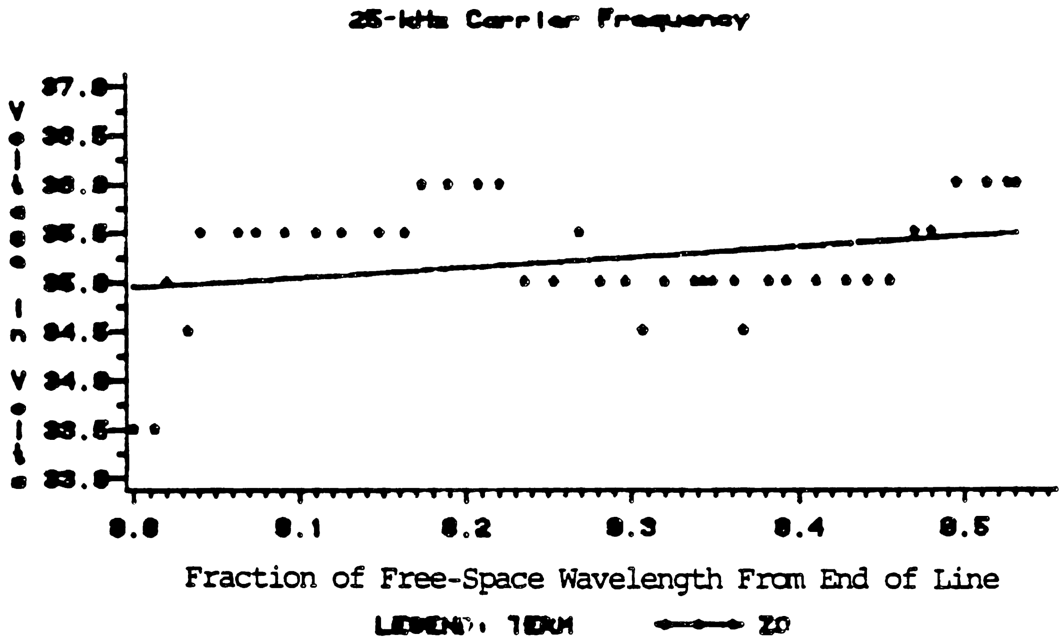

Figure 3.25 - Voltage attenuation for the distribution line terminated in 450 ohms (free-space wavelength = 11.44 miles)

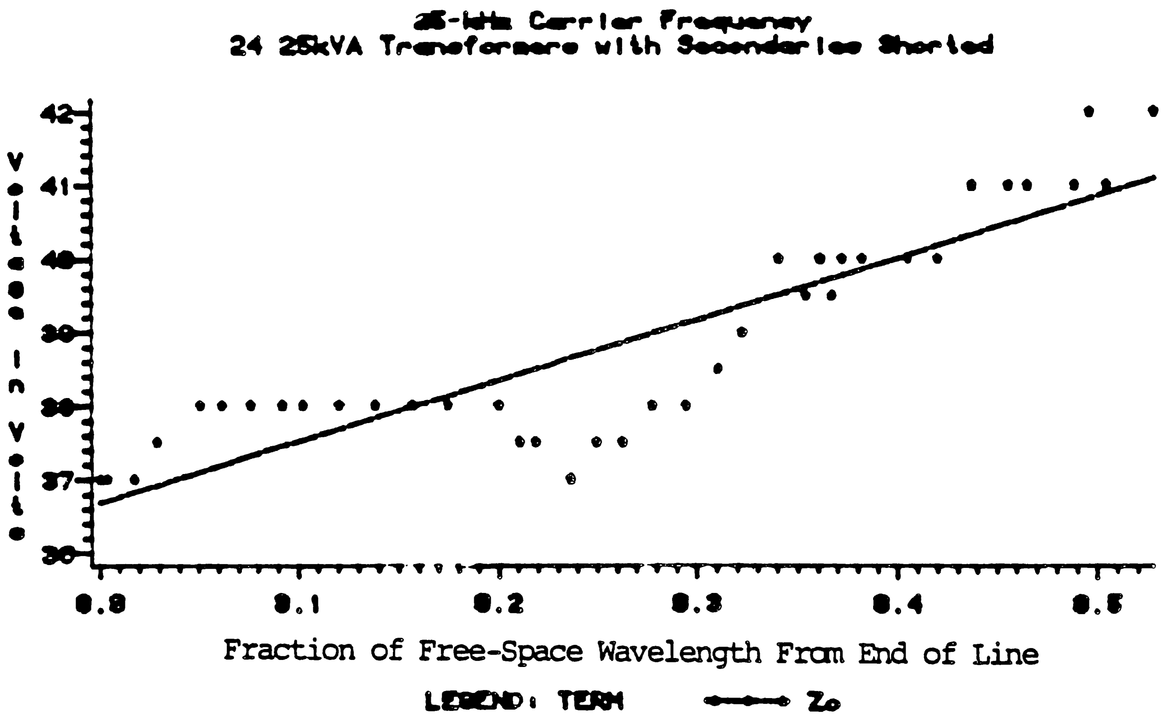

Figure 3.26 - Voltage attenuation for the distribution line with transformers, line terminated in 381 ohms, secondaries short circuited (free-space wavelength = 11.44 miles)

increasing the permittivity of the medium (and hence slowing down the velocity of propagation). The VSWR has remained at almost exactly 25 dB, although the node is not quite as sharply defined as it was in figure 3.17. The terminating resistance of 380 ohms was very successful in eliminating the standing-wave pattern, as exemplified by figures 3.21 and 3.22.

The impedance of the line has changed with the addition of the transformers. Comparing figure 3.23 with figure 3.19, it appears that the transformers have produced two significant effects. The transformers have doubled the width of the peak. However, the height of the peak has been decreased from around 7 kilohms to 3 kilohms. From a DLC transmission standpoint, this is an improvement because transmitters do not have to transmit into as high an impedance. When the line was terminated into 380 ohms, the impedance of the line was constant between 380 and 390 ohms. As one should expect, the addition of the transformers had no real impact on the neutral current. Any differences between figure 3.20 and 3.24 are expected to be the result of local changes in the earth's resistivity (the two sets of measurements were separated in time by over a three-week period).

One final calculation was made from the results of figures 3.17 and 3.21. With the line terminated into the respective characteristic impedance, the voltage vs. distance plots were expanded to obtain figures 3.25 and 3.26. With the Zo termination, no reflected wave is present and these plots show the actual attenuation of the voltage waveform as it travels down the distribution line. In figure 3.25, no transformers were attached to the line, and a loss of 34.9/35.5, or .148 dB was obtained over the 20,847 ft. section. This corresponds to a loss of approximately .04 dB per mile, an essentially insignificant figure. With the 24 transformers attached to this section the plot of figure 3.26 was obtained. The loss is now 36.7/41.1, or .25 dB per mile. This figure is still quite small, but should not be completely ignored. This agrees reasonably well the maximum per mile loss of .5 dB computed in section 3.2.

4. Conclusions

This paper has investigated the propagation of power line carrier signals on a power distribution line in the presence of distribution transformers. The classical RLCG distributed circuit model was modified to incorporate the effects of evenly spaced distribution transformers. Overall, a very general conclusion can be made. The addition of the distribution transformers simply adds capacitance to the distribution line, and all related parameters follow according to transmission line theory. Several specific conclusions that are important to the scope of this paper were drawn from the results and are enumerated as follows:

1. For the VLF frequency range, the unconnected power distribution line can be accurately modelled as a two-wire transmission line. This enables the use of standard transmission line theory for analyzing a plain distribution line.

2. The effect of distribution transformers can be incorporated into the distributed model of the distribution line. Equation's 2.20 to 2.22 can be used to calculate the effect of distribution transformers spaced at N transformers per mile.

3. The primary impedance of distribution transformers is affected by their secondary loads for frequencies below 25-kHz. In general, the phase of the primary impedance is more sensistive than the magnitude. With very few exceptions, the magnitude of the primary impedance is above 10 kohms. The phase of the impedance is predominately capacitive, and for frequecies above 20-kHz the phase is completely capacitive.

4. The magnitude of the primary impedance of the distribution transformers decreases slowly with increasing frequency. A resonance occurs in the 5 to 15-kHz range.

Carrier signal propagation measurements were made on a distribution line in a controlled environment. Measurements were made in both the frequency and the time domain. Furthermore, results were obtained for both the distribution line with transformers and for the distribution line by itself. From these results, several conclusions can be made:

5. The velocity of propagation on an unloaded distribution line is approximately 95 percent of the speed of light in air.

6. The addition of 6.1 distribution transformers per mile reduced the velocity of propagation to 85 percent of the speed of light in air. This is because the addition of

transformers has added capacitance to the line. The added capacitance increases the relative permitivity of the distribution line, therefore decreasing the the velocity of propagation.

7. The characteristic impedance of a distribution line is about 450 ohms. However, this value is not very sensitive as a tolerance of about 5 percent is acceptable.

8. The addition of the 6.1 transformers per mile lowered the characteristic impedance of the line to 381 ohms when the secondaries were short-circuited, and to 364 ohms when the secondaries were open-circuited.

9. The phase shift of the distribution line with and without transformers was found to be linear with frequency, with the slope increasing slightly with the addition of the transformers.

10. There appears to be very little loss on the line itself at the 25-kHz test frequency. This loss is on the order of .05 dB per mile. With the addition of the 6.1 transformers per mile the loss increased only slightly, to about .25 dB per mile

11. In these measurements, the current in the neutral conductor was usually less than 50 percent of the current in the phase conductor. This demonstrates that (at least

for the soil conditions at the distribution test site) the primary return path is the ground as opposed to the neutral conductor. This result is directly dependent on the earth's conductivity for the area under investigation.

12. Under this controlled environment, the greatest VSWR observed was approximately 27 dB for the distribution line by itself at 25-kHz. This figure decreased to about 25 dB with the addition of the 6.1 transformers per mile.

Additional research and measurements in some of these areas should be considered for future investigation. Further measurements of signal propagation on a distribution line with transformers at different spacings would be useful in documenting the effect of changes in transformer spacing. Likewise, it may prove useful to measure signal propagation with different size transformers. Another area that will probably see more research in the future is the propagation of carrier signals on the secondary side of the transformers (in addition to the transformer's transfer characteristics). As the distribution medium becomes clearer at frequencies other than 60 Hz, one may expect to see a substantial increase in communications on power distribution lines.

REFERENCES

1. Alder, R. B., Chu, L. J., and Fano, R. M., Electromagnetic Energy Transmission and Radiation, New York: John Wiley and Sons, Inc., 1960, pp. 58-105.

2. Burr, A. G., Burbidge, R. F., and Revett, J. E., "An Investigation of the Propagation of High Frequency Signals Over LV Mains Distribution Networks Using Computer Modelling and Direct Measurements," 4th International Conference, Metering Apparatus and Tariffs for Electricity Supply, IEE, London, October 1982.

3. Chen, Chao-Shun, "Energy Models of Power System Loads," Master's Thesis, University of Texas at Arlington, December 1981.

4. Davidson, C. W., Transmission Lines for Communications, New York: John Wiley and Sons, Inc., 1978, pp. 19-79.

5. "Field Demonstration of Communication Systems For Distribution Automation," Electric Power Research Institute, EL-1860, Vol. 1, Project 850, Final Report, March 1982.

6. Ghausi, M. S. and Kelly, J. J., Introduction to Distributed Parameter Networks with Application to Intregrated Circuits, New York: Holt, Rinehart, and Winston, Inc., 1968, pp. 1-25.

7. Grossner, N. R., Transformers for Electronic Circuits, New York: McGraw-Hill,

8. Hayt, W. H., Engineering Electromagnetics, New York: McGraw-Hill, 4th Edition, 1981, pp. 165-169,427-462,510.

9. Reference Data For Radio Engineers, New York: Howard W. Sams and Co., 1975, pp. 4-22.

10. Reinsch, C. H., "Smoothing by Spline Functions", Numerische Mathematik, 10, pp. 177-183 (1967).

11. "RF Model of the Distribution System as a Communication Channel," General Electric Co., Contract No. 955647, Phase II, Vol. 2, Task 4, July 28, 1982, pp. 1-76.

12. "RF Model of the Distribution System as a Communication Channel," General Electric Co., Contract No. 955647, Phase II, Vol. 3, Appendix 3, July 28, 1982, pp. 14-18.

13. Sander, K. F., and Reed, G. A. L., Transmission and Propagation of Electromagnetic Waves, England: Cambridge University Press, 1978, pp. 153-200.

14. Shuey, Ken C., "Distribution Transformers at Power-Line Carrier Frequencies," GLOBECOM: IEEE Global Telecommunications Conference, 1983, Vol. 1, pp. 483-486.

15. Spotts, T., E., "The Measurement and Analysis of High Frequency Noise on Distribution Lines," Master's Thesis, North Carolina State University, Raleigh, N.C., 1982, pp. 10-15.

16. "The Distribution Automation 23 kV Test Facility, An Introduction," Carolina Power and Light Company Introductory Report, Raleigh, N.C., May 16, 1984.

17. Van Valkenburg, M. E., Network Analysis, Englewood Cliffs, New Jersey: Prentice-Hall, Inc., 3rd Edition, 1974, pp. 325-351.

18. Woodruff, L. F., Principles of Electric Power Transmission, New York: John Wiley and Sons, Inc., 2nd Edition, 1956, pp. 72-90.